Integrable Models in Physics

Angela Foerster

Universidade Federal do Rio Grande do Sul

Instituto de Física, Porto Alegre

talk presented at "Quantum non-equilibrium phenomena"

June, Natal, 2016

Integrable Models:

Quantum models which can be exactly solved by Bethe Ansatz

IM can be found in different areas, such as:

- Statistical Physics

- Quantum Field Theory

- ***Condensed Matter

- ***Ultracold Atoms

Present some integrable models in CM and UA,
focusing on some prominent examples

OUTLINE

1- Introduction

2- Integrable models in Condensed Matter

- Spin ladder model

3- Integrable models in Ultracold Matter

- Bosonic quantum tunneling models

- Fermi gas with polarization

- Few particles system

4- Breaking the integrability

5- Conclusions

Main emphasis: results and physical properties

1 - INTRODUCTION

Importance of the study of integrable models:

- They serve as a test for computer analysis and analytic methods for realistic systems, where only numerical calculations and perturbative methods may be applied;

- They serve as a laboratory for investigations for the situations (1) where the mean field treatment fails (quantum fluctuations are large) or (2) which cannot be described via perturbation theory (strong coupling);

- From the mathematical point of view, they provide explicit realization of algebraic structures, such as Lie algebras and quantum groups;

Importance of the study of integrable models:

- From the experimental point of view, there are materials which behave like (quasi) 1D systems, such as $KCuF_3$, Sr_2CuO_3, $(C_5D_12N)_2CuBr_4$, $(5IAP_2CuBr_42H_2O)$, $Cu_2(C_5H_{12}N_2)_2Cl_4$, ... which can be well described by integrable spin chains and ladders;

- Some integrable systems have been realized in the lab in the context of ultracold atoms.

2 - Integrable models in Condensed Matter

Spin ladder systems

Importance:

Some compounds have been realized experimentally with a ladder structure:

$$SrCu_2O_3$$

$$La_{1-x}Sr_xCuO_2, 5$$

$$Sr_{14-x}Ca_xCu_24O_{41}$$

$$Cu_2(C_5H_{12}N_2)Cl_4$$

$$CaV_2O_5$$

$$KCuCl_3$$

- Different experiments using these compounds do report on the existence of a spin gap in the energy spectrum: *magnetic susceptibility, NMR techniq.*

- In some of these even leg-ladder compounds superconductivity has been detected upon hole doping (chemical substitution)
  detected in resistivity curves

- It has been observed that:
  Even leg ladders exhibit a gap;
  Odd leg ladders do not exhibit a gap.

DEFINITION: Spin ladder
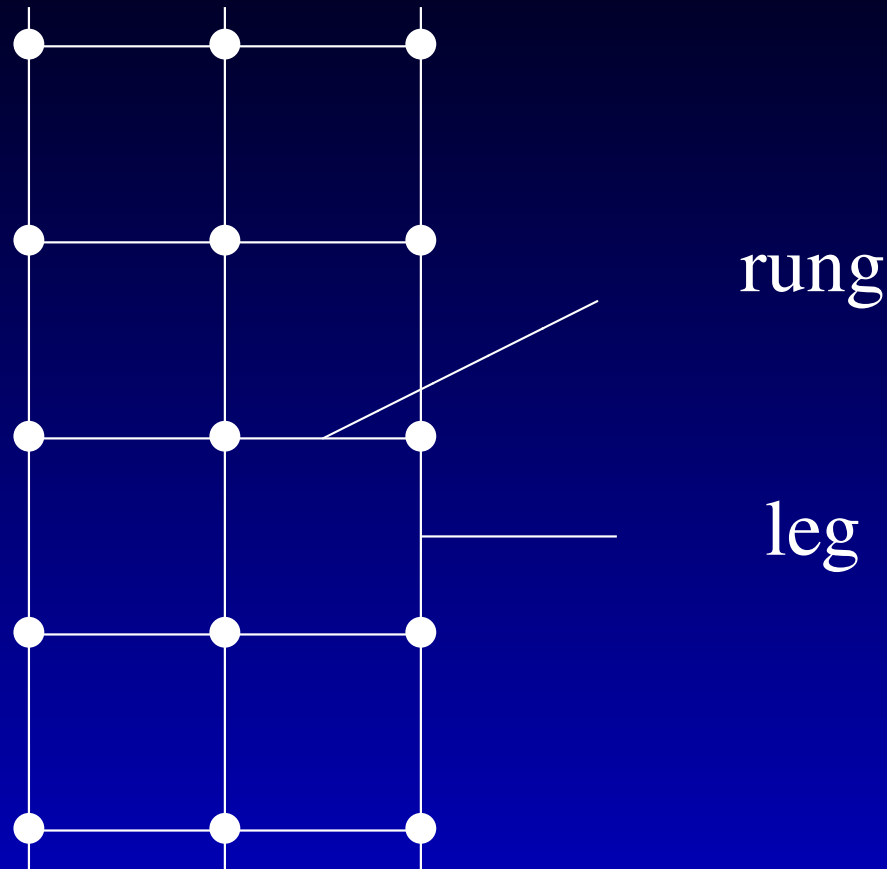
- *construction: put some 1D spin chains together, in such a way that the n^o of legs (L) $<< n^o$ of rungs*

- *interpolates between 1 and 2 dimensions*

- *historically, the name came from the 2-legs, and it was extended after for n-legs*

A SIMPLE INTEGRABLE SPIN LADDER MODEL:

$$\mathcal{H} = \frac{J_\parallel}{\gamma}\,\mathcal{H}_{\text{leg}} + J_\perp \sum_{j=1}^{L} \vec{S}_j \vec{T}_j - \mu_B g H \sum_{j=1}^{L}(S_j^z + T_j^z),$$

$$\mathcal{H}_{\text{leg}} = \sum_{j=1}^{L}\left(\vec{S}_j\vec{S}_{j+1} + \vec{T}_j\vec{T}_{j+1} + 4\,\vec{S}_j\vec{S}_{j+1}\vec{T}_j\vec{T}_{j+1}\right)$$

Yupeng Wang PRB60 (1999)

- S_j, T_j are Pauli matrices acting on site j of the left and right legs

- $J_\parallel$ and $J_\perp$ are the leg and and rung couplings and γ is a rescaling constant

- H is the magnetic field, L is the number of rungs and PBC are imposed

- It differs from the usual Heisenberg ladder by the presence of biquadratic interactions
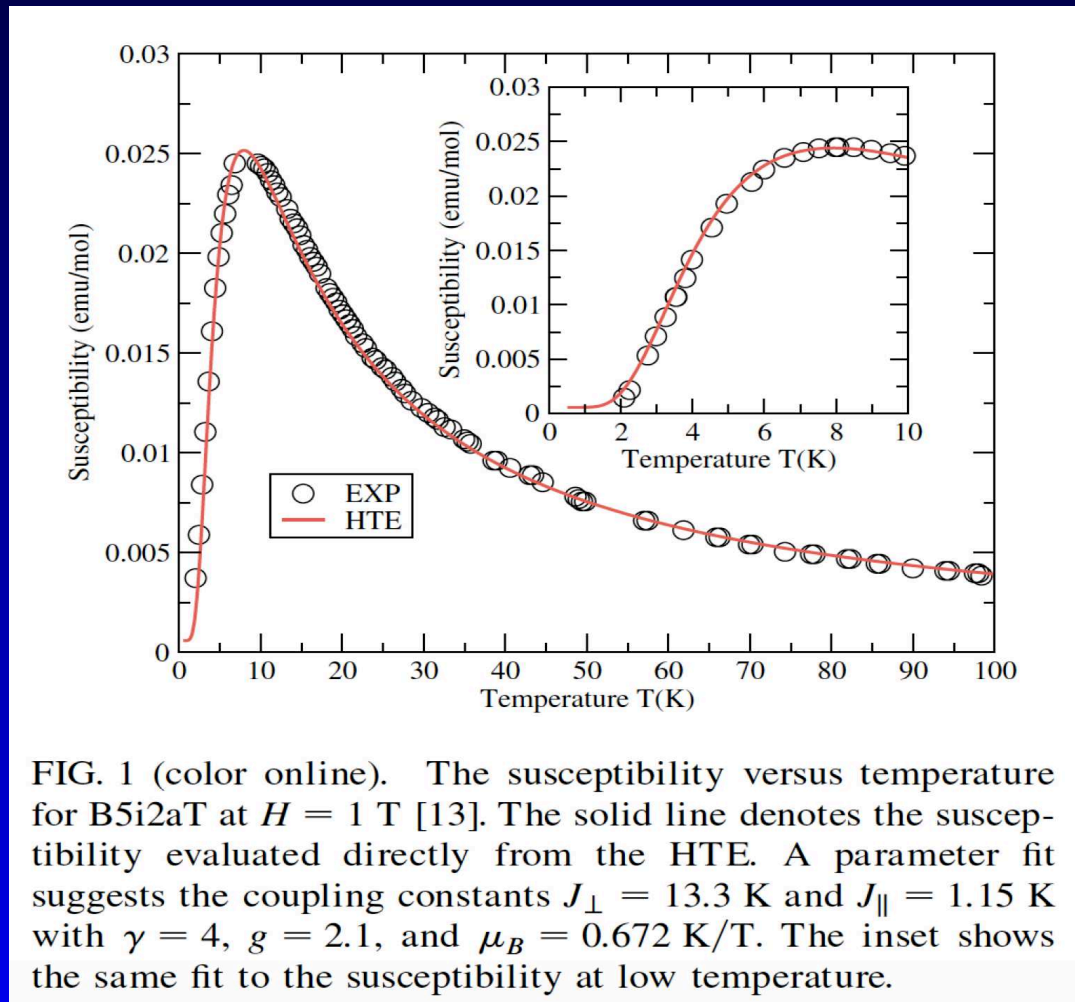
Properties:

- this model can be exactly solved by the BA:

  the leg part is simply the permutation operator corresponding to the $su(4)$ algebra and the rung term becomes diagonal after a convenient change of basis;

- the gap and critical fields can be derived using the TBA;

- the thermal and magnetic properties can be obtained using the Quantum Transfer Matrix (QTM) method:

  the free energy is written in terms of the eigenvalue of the QTM and from it we derive the thermodynamical properties by standard thermodynamics;

- this integrable ladder model can be used to describe the physics of some strong coupling ladder compounds.

Comparison with experimental curves:

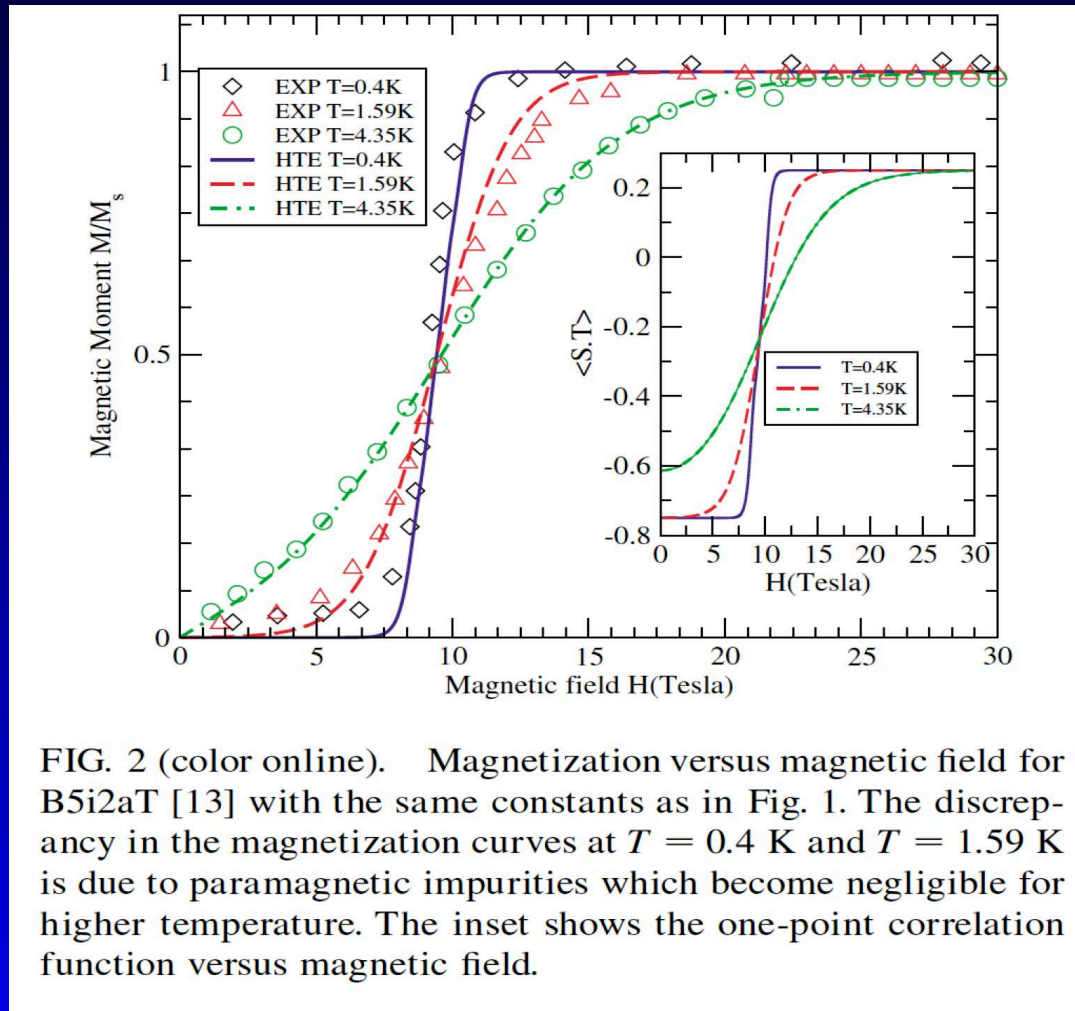We can use this integrable spin ladder model to fit experimental curves
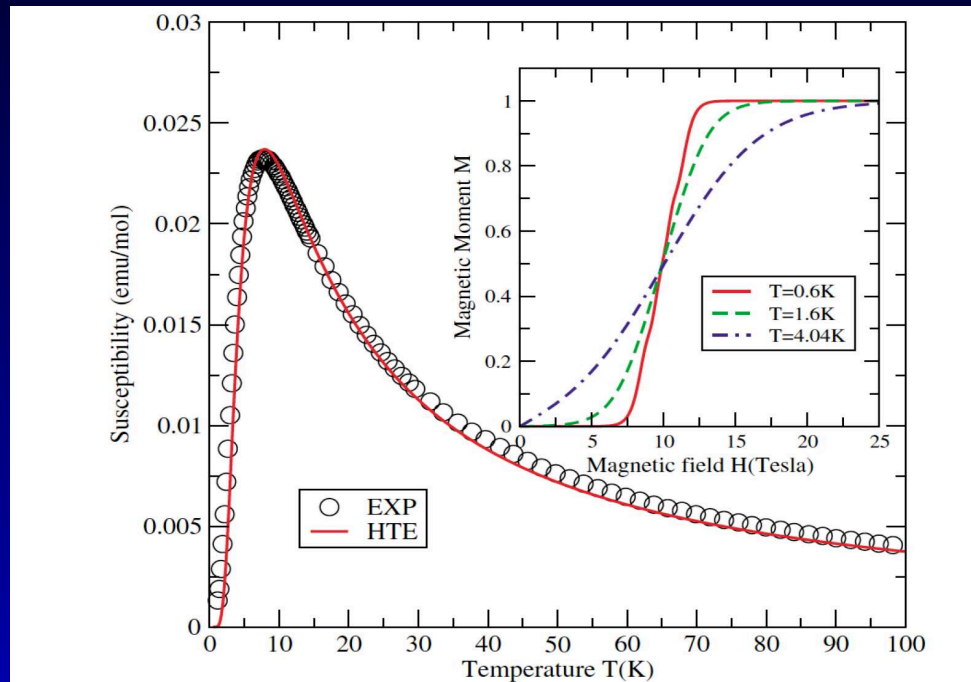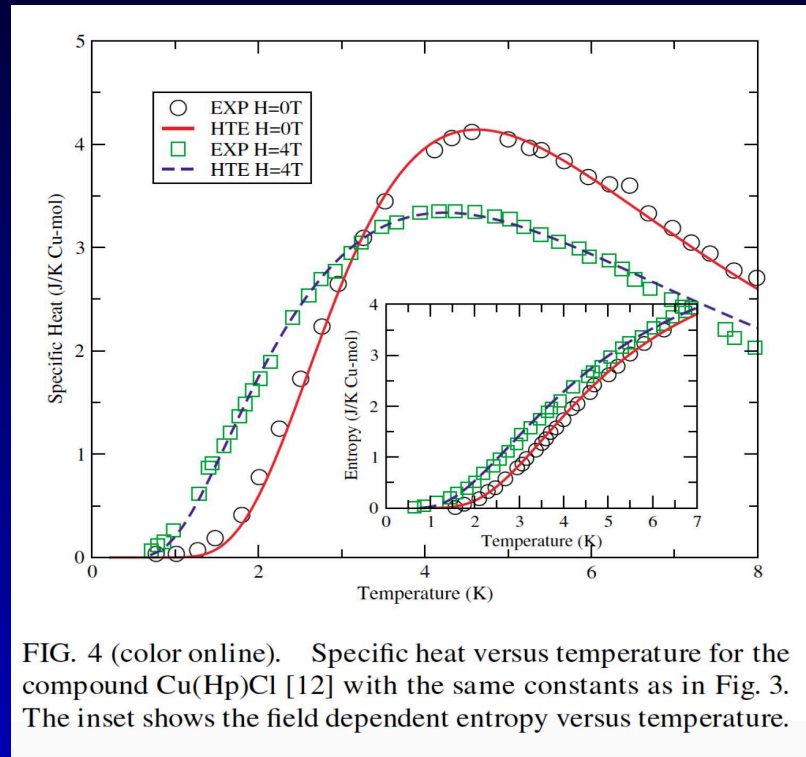
- $(5IAP_2CuBr_42H_2O)$

FIG. 1 (color online). The susceptibility versus temperature for B5i2aT at $H = 1$ T [13]. The solid line denotes the susceptibility evaluated directly from the HTE. A parameter fit suggests the coupling constants $J_\perp = 13.3$ K and $J_\parallel = 1.15$ K with $\gamma = 4$, $g = 2.1$, and $\mu_B = 0.672$ K/T. The inset shows the same fit to the susceptibility at low temperature.

C. Landee, PRB63 (2001); M. Batchelor et al, PRL (2003)

Comparison with experimental curves:

- $(5IAP_2CuBr_42H_2O)$

FIG. 2 (color online). Magnetization versus magnetic field for B5i2aT [13] with the same constants as in Fig. 1. The discrepancy in the magnetization curves at $T = 0.4$ K and $T = 1.59$ K is due to paramagnetic impurities which become negligible for higher temperature. The inset shows the one-point correlation function versus magnetic field.

C. Landee, PRB63 (2001); M. Batchelor et al, PRL (2003)

Comparison with experimental curves:

- $Cu_2(C_5H_{12}N_2)_2Cl_4$

FIG. 3 (color online). Susceptibility versus temperature for the compound Cu(Hp)Cl [12]. The solid line denotes the susceptibility evaluated directly from the HTE with $\mu_B = 0.672$ K/T, $J_\perp = 13.5$ K, $J_\parallel = 2.4$ K, $\gamma = 5$, and $g = 2.03$. The inset shows the magnetization versus magnetic field at different temperature. At $T = 0.6$ K, the critical fields are $H_{c1} \approx 7.8$ T and $H_{c2} \approx 13.0$ T, in good agreement with the experimental results [11,12].

M. Hagiwara et al, PRB62 (2000); M. Batchelor et al, PRL (2003)

Comparison with experimental curves:

- $Cu_2(C_5H_{12}N_2)_2Cl_4$

FIG. 4 (color online). Specific heat versus temperature for the compound Cu(Hp)Cl [12] with the same constants as in Fig. 3. The inset shows the field dependent entropy versus temperature.

M. Hagiwara et al, PRB62 (2000); M.Batchelor, PRL (2003)

Excellent agreement is found between the theoretical results and the experimental data for these ladder compounds

Other integrable models in Condensed Matter

- Heisenberg chain

- Susy t-J model

- Hubbard model

- Kondo lattice and other impurity models

- . . .

3 - Integrable models in Ultracold Matter

Bosonic quantum tunneling models:

- 2 wells: Two-site Bose Hubbard Hamiltonian

- 3 wells: Triple well Hamiltonian

- 4 wells: Four-well ring model

- ....

- Multi-well tunneling models

Two-site Bose Hubbard Hamiltonian:

$$H = \frac{K}{8}(N_1 - N_2)^2 - \frac{\Delta\mu}{2}(N_1 - N_2) - \frac{\mathcal{E}_J}{2}(a_1^\dagger a_2 + a_2^\dagger a_1)$$

- $N_i = a_i^\dagger a_i$: number of atoms in well $(i = 1, 2)$

- K: atom-atom interaction term

- $\Delta\mu$: external potential

- $\mathcal{E}_J$: tunneling strength

*G. Milburn et al, Phys. Rev. A **55** (1997) 4318; A. Leggett, Rev. Mod. Phys. **73** (2001) 307*

A. Tonel, J. Links, A. Foerster, JPA 38 (2005) 1235

The quantum dynamics of the model exhibits tunneling X
self-trapping - experiment of Albiez et al - 2005

Quantum Dynamics:

Time evolution of the expectation value of the imbalance population $(N_1 - N_2)/N$ for different ratios of the coupling $K/\mathcal{E}_J$ and $\Delta\mu = 0$ and initial state $|N, 0>$
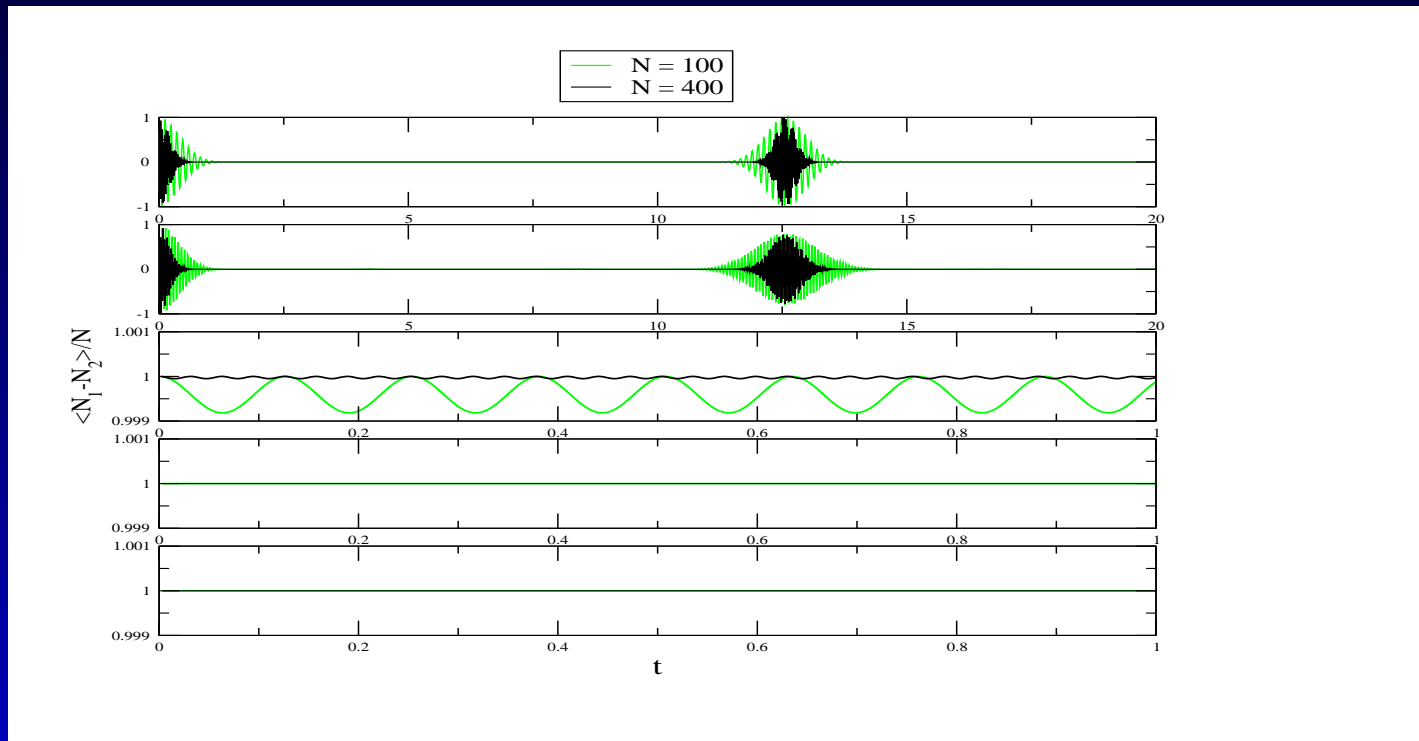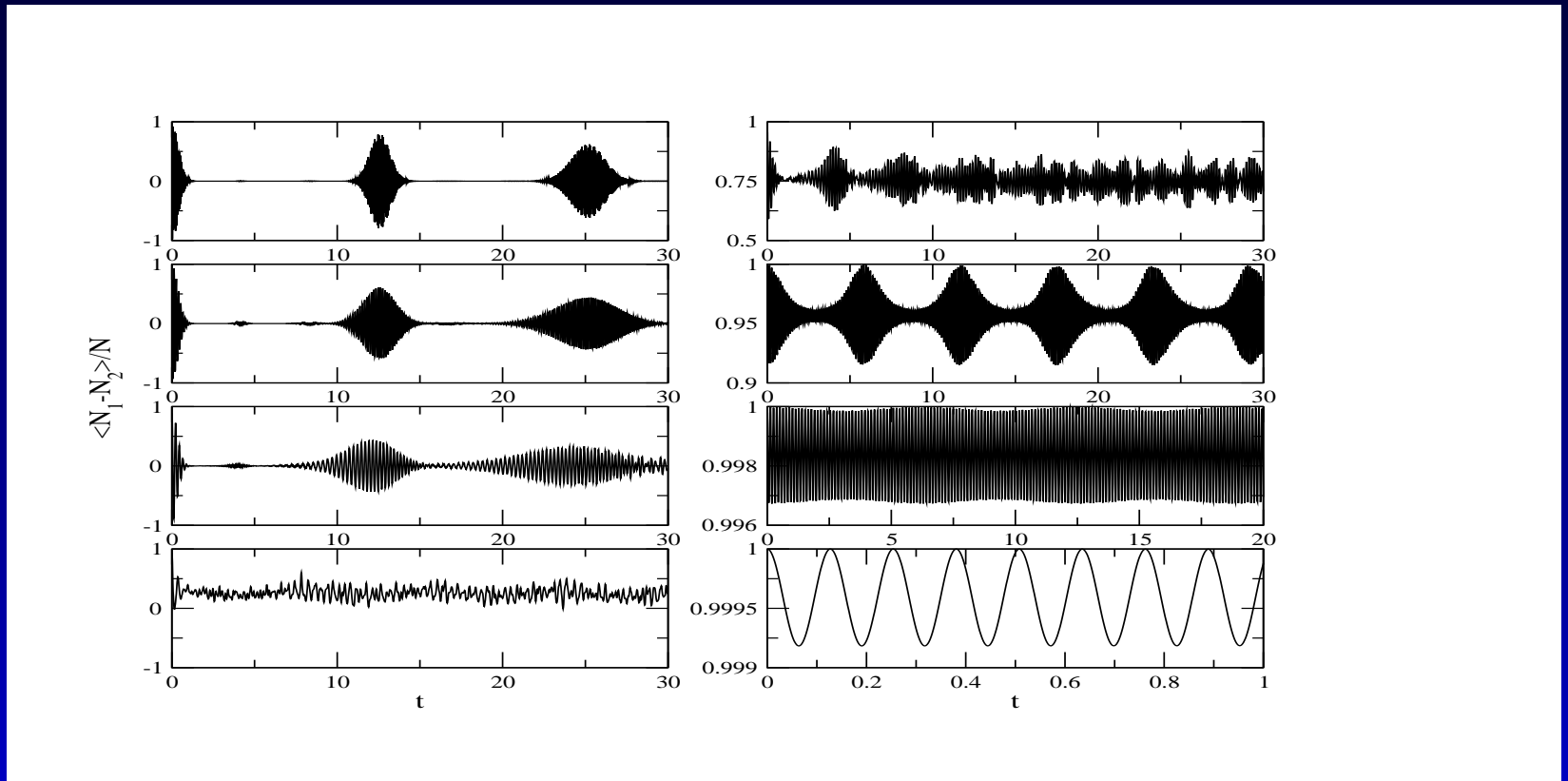

$$\frac{K}{\mathcal{E}_J} = \frac{1}{N^2}, \quad \frac{1}{N}, \quad 1, \quad N, \quad N^2$$

- the qualitative behaviour does not depend on the number of particles;
- collapse and revival behaviour, typical of the experiments;
- between $\frac{K}{\mathcal{E}_J} = \frac{1}{N}$ and 1 the system tends to localize

Quantum Dynamics:

Time evolution of the expectation value of the imbalance population $(N_1 - N_2)/N$ for different ratios of the coupling $K/\mathcal{E}_J$ and $\Delta\mu = 0$

$$\frac{K}{\mathcal{E}_J} = \frac{1}{N}, \quad \frac{2}{N}, \quad \frac{3}{N}, \quad \mathbf{\frac{4}{N}}, \quad \frac{5}{N}, \quad \frac{10}{N}, \quad \frac{50}{N}, \quad \mathbf{1}$$

$$\frac{K}{\mathcal{E}_J} = \frac{4}{N}: \text{Tunneling X Self-trapping}$$

Direct observation of tunneling and self-trapping:
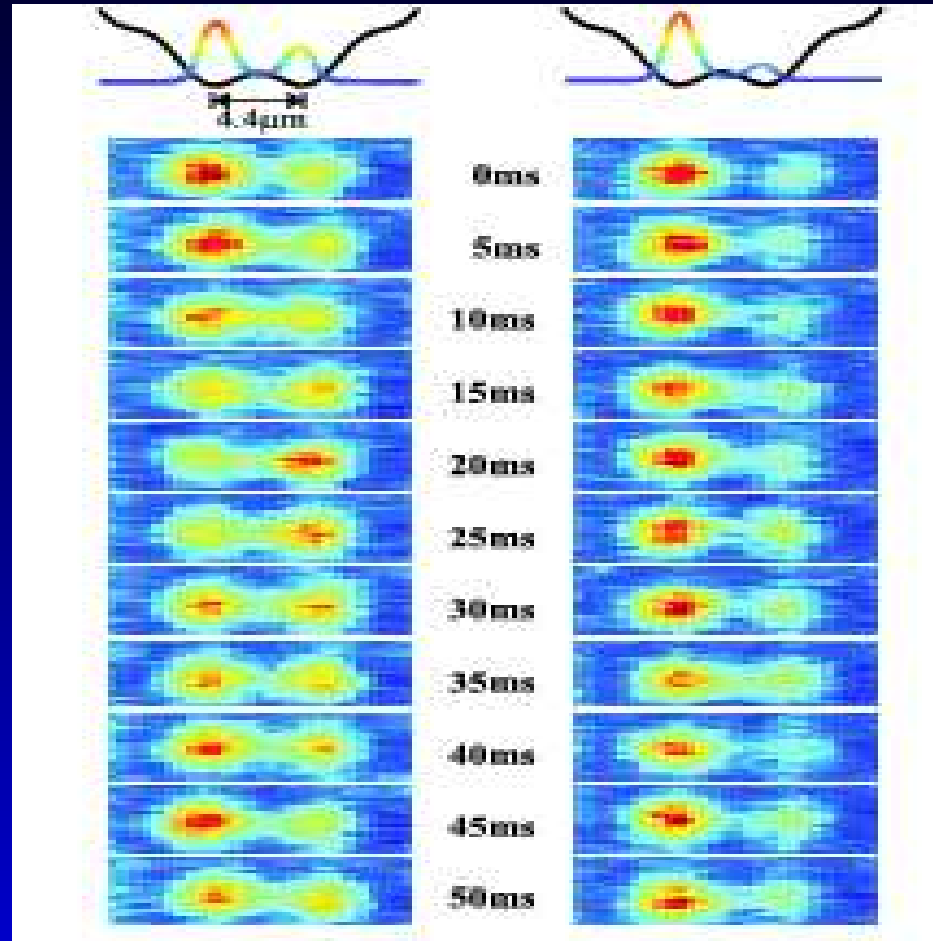
Albiez, M. et al., Phys. Rev. Lett. **95** (2005) 010402

The two-site Bose Hubbard model describes qualitatively tunneling X self-trapping

Integrability and exact solution:

- R-matrix:

$$R(u) = \begin{pmatrix} 1 & 0 & 0 & 0 \\ 0 & b(u) & c(u) & 0 \\ 0 & c(u) & b(u) & 0 \\ 0 & 0 & 0 & 1 \end{pmatrix},$$

$$b(u) = \frac{u}{u + \eta} \qquad c(u) = \frac{\eta}{u + \eta}$$

- Yang-Baxter algebra:

$$R_{12}(x-y)R_{13}(x)R_{23}(y) = R_{23}(y)R_{13}(x)R_{12}(x-y)$$

- Monodromy-matrix:

$$T(u) = \begin{pmatrix} A(u) & B(u) \\ C(u) & D(u) \end{pmatrix}$$

- Yang-Baxter algebra:

$$R_{12}(u-v)T_1(u)T_2(v) = T_2(v)T_1(u)R_{12}(u-v)$$

- Realization of the monodromy matrix:

$$L(u) = \pi(T(u)) = L_1^a(u+w)L_2^a(u-w)$$

$$L_i^a(u) = \begin{pmatrix} u + \eta N_i & a_i \\ a_i^\dagger & \eta^{-1} \end{pmatrix} \qquad i = 1,2$$

- Transfer matrix:

$$\tau(u) = \pi(Tr(T(u))) = \pi(A(u) + D(u))$$

- Integrability:

$$[\tau(u), \tau(v)] = 0 \longrightarrow [H, \tau(v)] = 0$$

- Hamiltonian and transfer matrix:

$$H = \kappa \left(\tau(u) - \frac{1}{4}(\tau'(0))^2 - u\tau'(0) - \eta^{-2} + w^2 - u^2 \right)$$

with the identification:

$$\frac{K}{4} = \frac{\kappa\eta^2}{2}, \qquad \frac{\Delta\mu}{2} = -\kappa\eta w, \qquad \frac{\mathcal{E}_{\mathcal{J}}}{2} = \kappa$$

$$H = \frac{K}{8}(N_1 - N_2)^2 - \frac{\Delta\mu}{2}(N_1 - N_2) - \frac{\mathcal{E}_J}{2}(a_1^\dagger a_2 + a_2^\dagger a_1)$$

Applying the algebraic Bethe ansatz method:

- Energy:

$$E = -\kappa \left(\eta^{-2} \prod_{i=1}^{N} \left(1 + \frac{\eta}{v_i - w} \right) - \frac{\eta^2 N^2}{4} - w \eta N - \eta^{-2} \right)$$

- Bethe Ansatz Equations:

$$\eta^2 (v_i^2 - w^2) = \prod_{j \neq i}^{N} \frac{v_i - v_j - \eta}{v_i - v_j + \eta}$$

INTEGRABLE GENERALISED MODELS:

Basic idea:

We can construct integrable generalised models in this bosonic quantum tunneling context by exploring different representations of some algebra.

*A. Foerster and E. Ragoucy*, Nuclear Phys. **B777** (2007) 373

A. Tonel, L. Ymai, A. Foerster and J. Links, J. Phys. **A48** (2015)

L. Ymai, A. Tonel, A. Foerster and J. Links, arXiv:1606.00816 (2016)

Triple well Hamiltonian:

$$
\begin{aligned}
H \;=\;& U(N_1 + N_3 - N_2)^2 + \mu(N_1 + N_3 - N_2) \\
& +\; t_{12}(a_1^\dagger a_2 + a_1 a_2^\dagger) + t_{23}(a_2^\dagger a_3 + a_2 a_3^\dagger)
\end{aligned}
\tag{1}
$$

- $N_i = a_i^\dagger a_i$: number of bosons in well i, $(i = 1, 2, 3)$,

  $N = N_1 + N_2 + N_3$ is constant, H is invariant by changing the indices 1 and 3

- U: controls on-site and inter-well interac. bet. bosons

- μ: external potential, t_{ij}: tunneling strength:
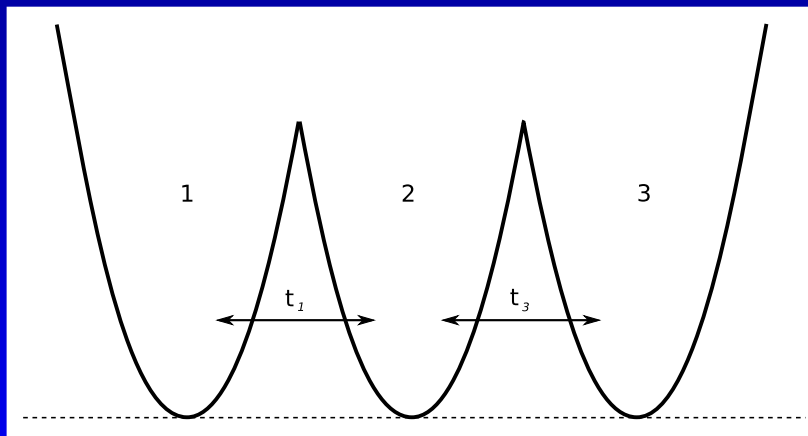
A. Foerster, J. Links, K. Wilsmann, A. Tonel and L. Ymai, in preparation (2016)

Four-well ring with anisotropic tunneling:

$$
\begin{aligned}
H \;=\;\; & U(N_1 + N_3 - N_2 - N_4)^2 + \mu(N_1 + N_3 - N_2 - N_4) \quad (2) \\
+ \;\; & t_{12}(a_1 a_2^\dagger + a_1^\dagger a_2) + t_{14}(a_1 a_4^\dagger + a_1^\dagger a_4) \\
+ \;\; & t_{23}(a_3 a_2^\dagger + a_3^\dagger a_2) + t_{34}(a_3 a_4^\dagger + a_3^\dagger a_4)
\end{aligned}
$$

t_{ij} are not independent: $t_{12}t_{34} = t_{23}t_{14}$ but still admits sufficient freedom to investigate a range

of anisotropic tunneling regimes
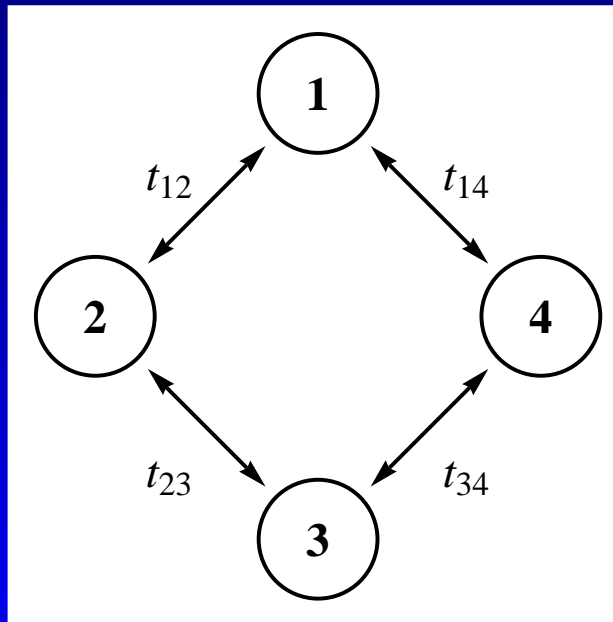
Yang-Baxter equation: key ingredient in this construction

$$R_{12}(x - y)R_{13}(x)R_{23}(y) = R_{23}(y)R_{13}(x)R_{12}(x - y)$$

- sufficient condition for integrability, proposed independently in different contexts by:

- C. N. Yang (China): Nobel Prize 1957

- R. Baxter (ANU, Australia): Boltzman Medal 1980, Lars Onsager Prize 2006, Royal Medal 2013

Experimental realization of the YBE using NMR:

SCIENTIFIC **REP🜨RTS**

OPEN **Experimental realization of the Yang-Baxter Equation via NMR interferometry**

Received: 19 October 2015
Accepted: 12 January 2016
Published: 10 February 2016

F. Anvari Vind[1,2], A. Foerster[2], I. S. Oliveira[1], R. S. Sarthour[1], D. O. Soares-Pinto[3], A. M. Souza[1] & I. Roditi[1]

The Yang-Baxter equation is an important tool in theoretical physics, with many applications in different domains that span from condensed matter to string theory. Recently, the interest on the equation has increased due to its connection to quantum information processing. It has been shown that the Yang-Baxter equation is closely related to quantum entanglement and quantum computation. Therefore, owing to the broad relevance of this equation, besides theoretical studies, it also became significant to pursue its experimental implementation. Here, we show an experimental realization of the Yang-Baxter equation and verify its validity through a Nuclear Magnetic Resonance (NMR) interferometric setup. Our experiment was performed on a liquid state Iodotrifluoroethylene sample which contains molecules with three qubits. We use Controlled-transfer gates that allow us to build a pseudo-pure state from which we are able to apply a quantum information protocol that implements the Yang-Baxter equation.

talk by Fatima Anvari
NMR-Group: coordinated by Ivan Oliveira, CBPF

Ultracold Fermi gases

1D 2-component attractive Fermi gas with polarization:

- Hamiltonian

$$\mathcal{H} = -\frac{\hbar^2}{2m}\sum_{i=1}^{N}\frac{\partial^2}{\partial x_i^2} + g_{1D}\sum_{1 \le i < j \le N}\delta(x_i - x_j) - \frac{H}{2}(N_\uparrow - N_\downarrow)$$

  - N spin $1/2$ fermions of mass m

  - constrained by PBC to a line of length L

  - H: external field

  - $g_{1D} = \frac{\hbar^2 c}{m}$: 1D interaction strength:
    attractive for $g_{1D} < 0$ and repulsive for $g_{1D} > 0$

  - Here: attractive regime

Properties:

- this model can be exactly solved by the BA

  *C.N. Yang, PRL **19**(1967)1312; M. Gaudin, Phys. Lett. **24** (1967) 55*

- using the TBA we can derive thermodynamical properties and also obtain the phase diagram for strong and weak coupling.

- using the TBA, we can also obtain the Wilson ratio R_W, an universal quantity defined as the ratio of the magnetic susceptibility χ to specific heat c_v divided by T (in the strong attractive and low T regime)
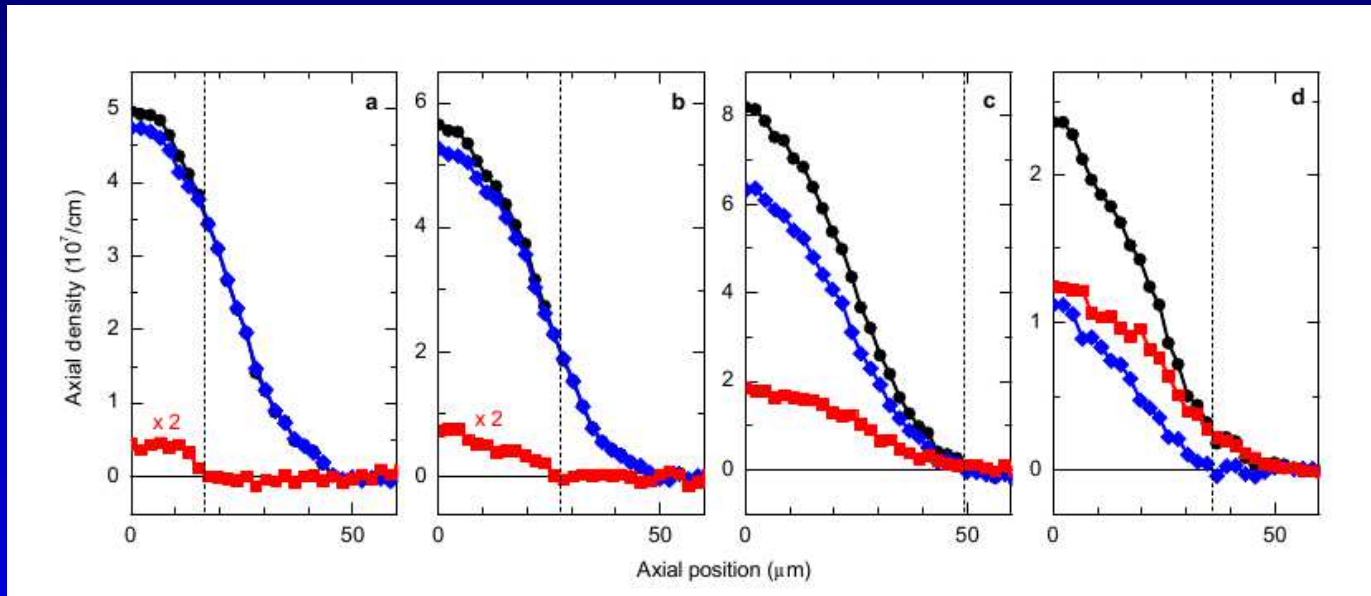
$$R_W \propto \frac{\chi}{c_v/T}$$

# Phase diagram ($T=0$) and schematic rep. (strong coupling)
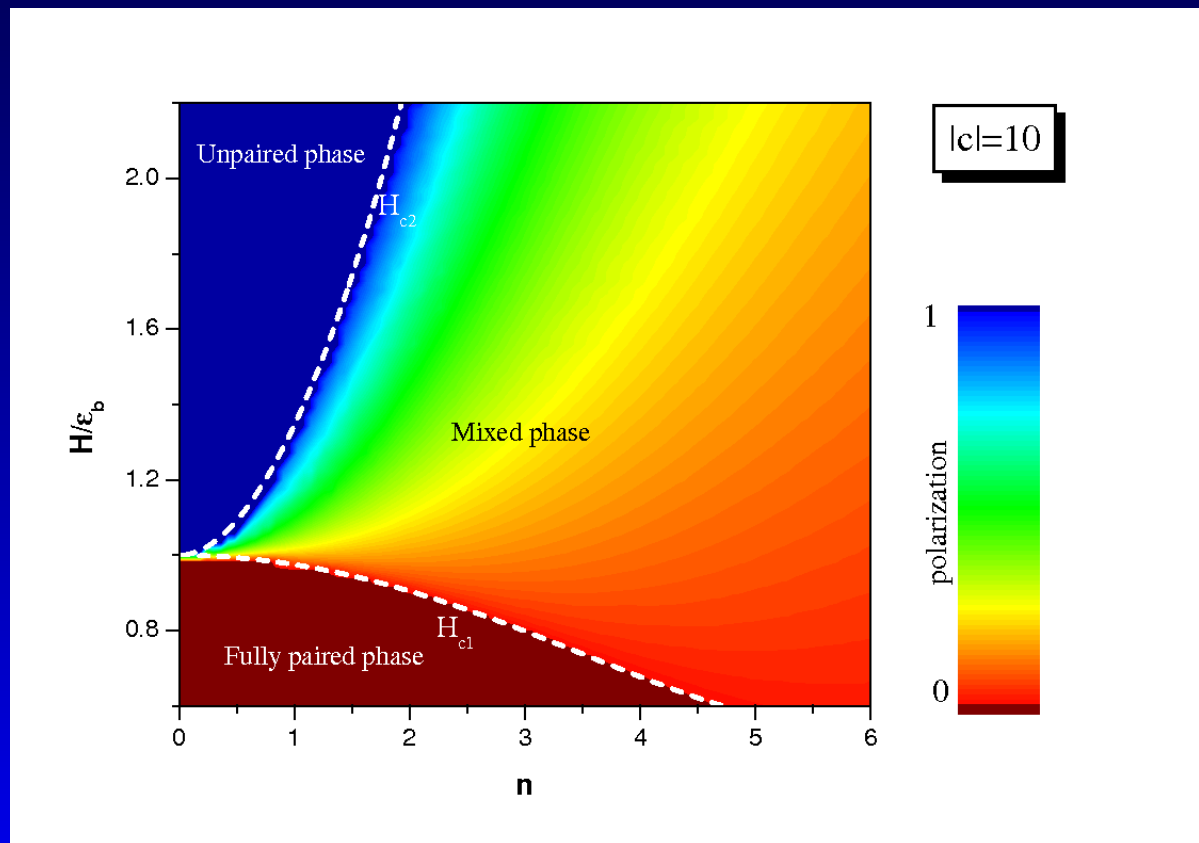
He, Foerster, Guan, Batchelor, NJP2009

- For low T: Theoretical predictions from low-T TBA + LDA (solid lines) in the strong coupling regime are in quantitative agreement with experimental measurements (circles) of density profiles of a 2-spin mixture of ultracold ^{6}Li atoms in 1D tubes


Liao et al. Nature 2010; the black (blue) circles are the density of fermions in the state $|1>$ $(|2>)$ and the red squares the difference between these two states; the solid lines are the predictions from TBA+LDA; the polarizations are 0.015, 0.055, 0.10 and 0.33

Contour Plot of the Wilson Ratio:
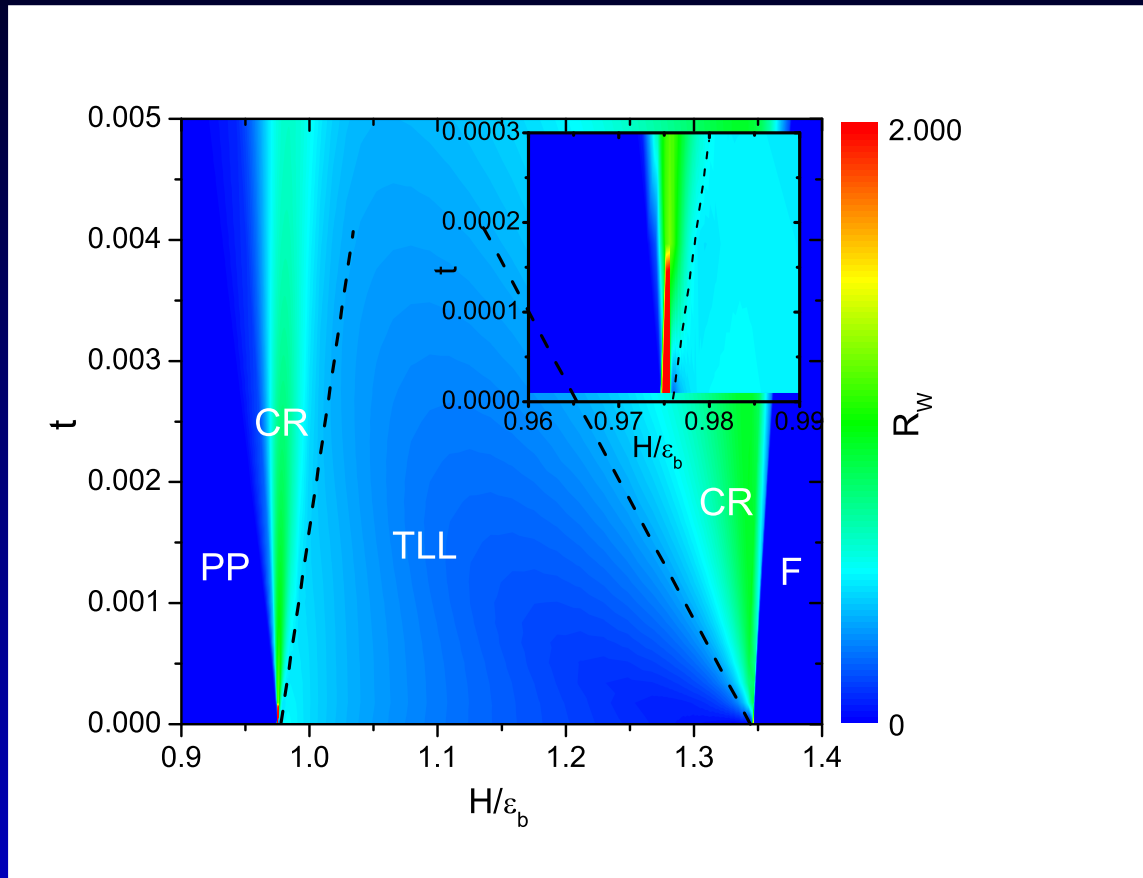
Contour plot of R_W for $|\gamma| = 10$ as a function of the temperature and magnetic field using the TBA. In the region below the dashed lines, R_W is temperature independent. $R_W = 0$ for the paired (PP) and ferromagnetic (F) phases. Near the critical points, the ratio reveals anomalous enhancement. The inset shows the enhancement at the lower critical point.

Wilson Ratio:
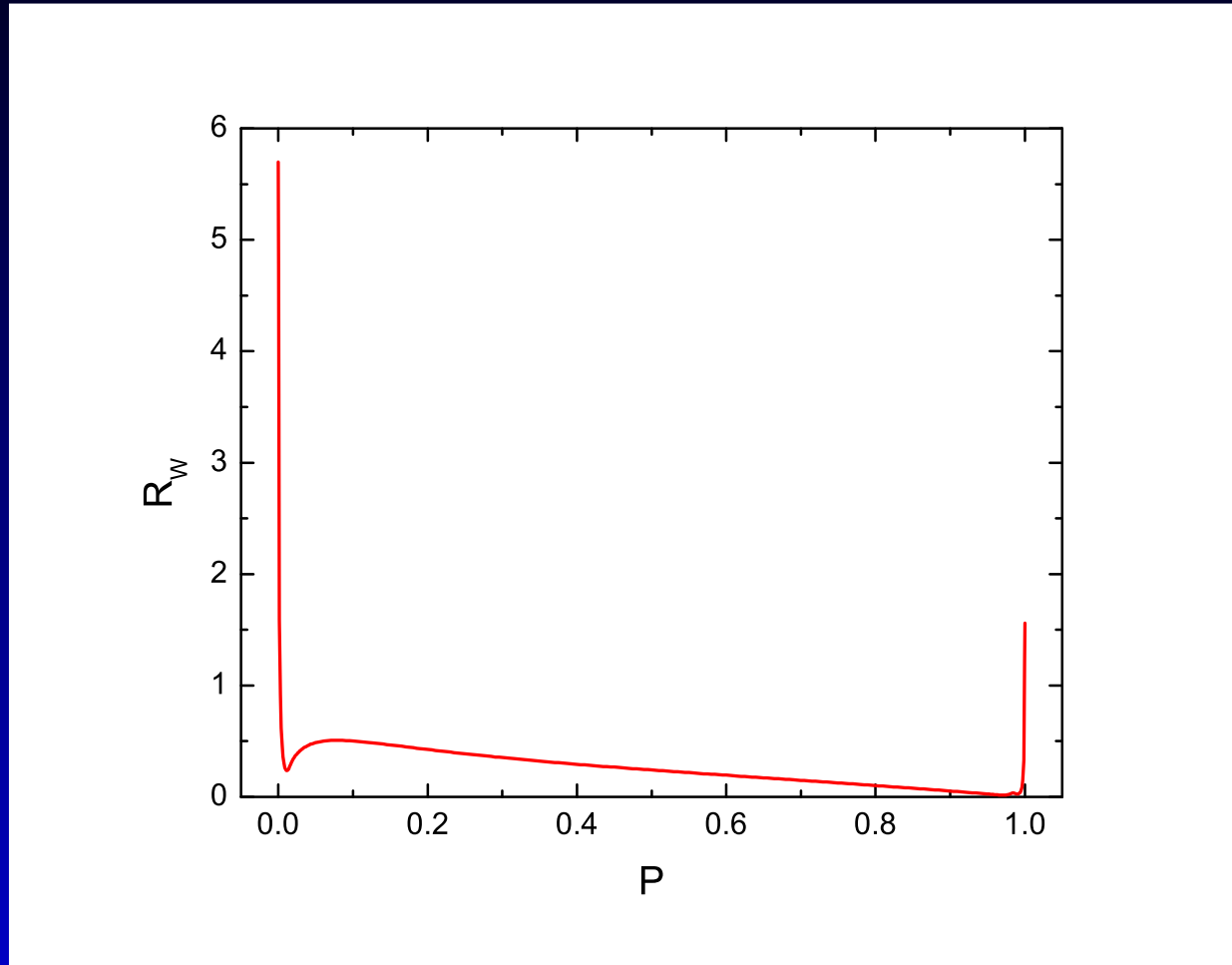
R_W vs polarization for $|\gamma| = 10$ at $T = 0.00001\epsilon_b$. The ratio exhibits anomalous enhancement near the two critical points due to the sudden change of the density of states. The values $R_W = 5.53$ and $R_W = 1.52$ agree with the values obtained from the analytic expression.

Guan, Yin, Foerster, Batchelor, Lee, Lin, PRL 2013

Other integrable models in Ultracold Matter

Advanced experimental techniques in trapping and cooling atoms in 1D have provided the realization of integrable models in the lab. Some examples:

- ## the Lieb-Liniger Bose gas
  T. Kinoshita et al Science 2004, PRL 2005, Nature 2006; A. van Amerongen et al PRL2008; T. Kitagawa et al PRL 2010; J. Armijo et al PRL 2010, H. Naegerl et al, 2015

- ## the super Tonks-Girardeau gas
  E. Haller et al Science 2009

- ## the two-component spinor Bose gas
  J. van Druten et al arXiv:1010.4545

- ## McGuire impurity model in 1D Fermi gas
  S. Jochim et al, Science 2011, PRL 2012, Science 2013.

- Even if a system is not integrable
  we can get inspiration from these methods;

- We can see this, for instance in the case of few
  particles systems, which are attracting great
  interest due to recent experiments in cold atoms.

Few particles

Few Particles System:

- Very recent experiments: Jochim et al prepared and controlled with high precision a system of few ^{6}Li atoms (N) in a 1D harmonic trap - Science 2012
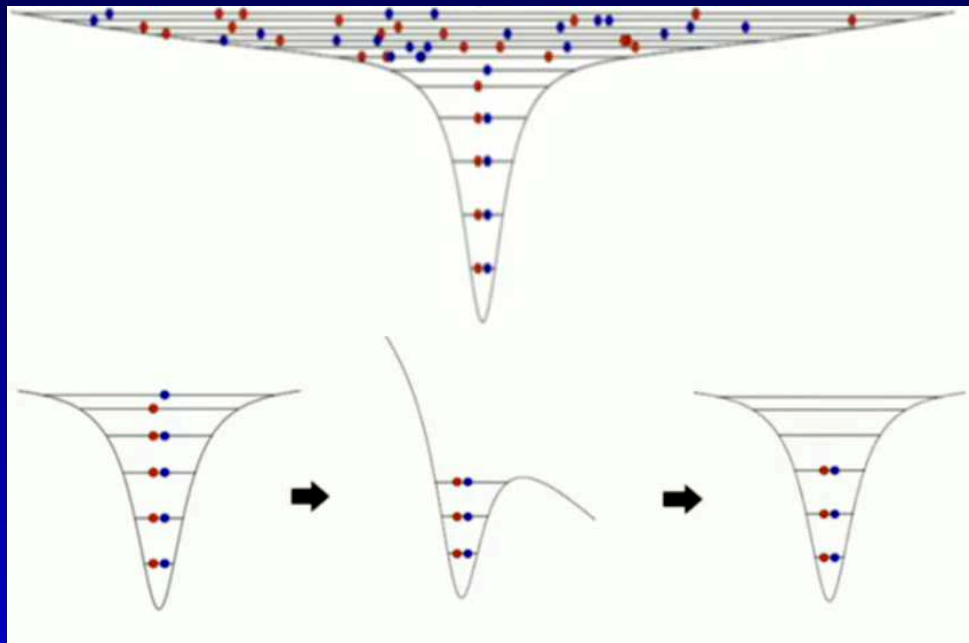
Microtrap + tilting the potential

Combining the Bethe ansatz + variational principle we discuss few particles system

Few-particles system in a 1D harmonic trap:

MOTIVATION: *Recent experiments on a system of few atoms in a 1D harmonic trap stimulated the search for new theoretical methods to deal with few-particles systems.*

$$\mathcal{H} = -\frac{\hbar^2}{2m} \sum_{i=1}^{N} \frac{\partial^2}{\partial x_i^2} + c \sum_{1 \leq i < j \leq N} \delta(x_i - x_j) + \frac{1}{2} \sum_{i=1}^{N} m\omega^2 x_i{}^2$$

- Few bosons N interacting via a delta-function in an axially symmetric harmonic trap with angular frequency w;

- c is the interaction strength, attractive for $c < 0$ and repulsive for $c > 0$

- The harmonic potential term prevents the exact solvability of $\mathcal{H}$. If we consider just the interaction Hamiltonian $(\omega = 0)$ it is exactly solvable by the Bethe ansatz

$$\mathcal{H} = -\frac{\hbar^2}{2m} \sum_{i=1}^{N} \frac{\partial^2}{\partial x_i^2} + g_{1D} \sum_{1 \le i < j \le N} \delta(x_i - x_j) + \frac{1}{2} \sum_{i=1}^{N} m\omega^2 x_i{}^2$$

- $N = 2$:

  exact analytical solution *- Th. Busch et al, Found.Phys. 1998*

- $N \ge 3$:

  no exact solution is available; BA + LDA is not possible!

- Our approach: by combining the Bethe ansatz with the variational principle, we calculate the GS-energy of the system with good agreement with the analytical result for $N = 2$ and numerical results for $N = 3$.

  The central part of the *trial function is the BA-wavefunction for the integrable model.*
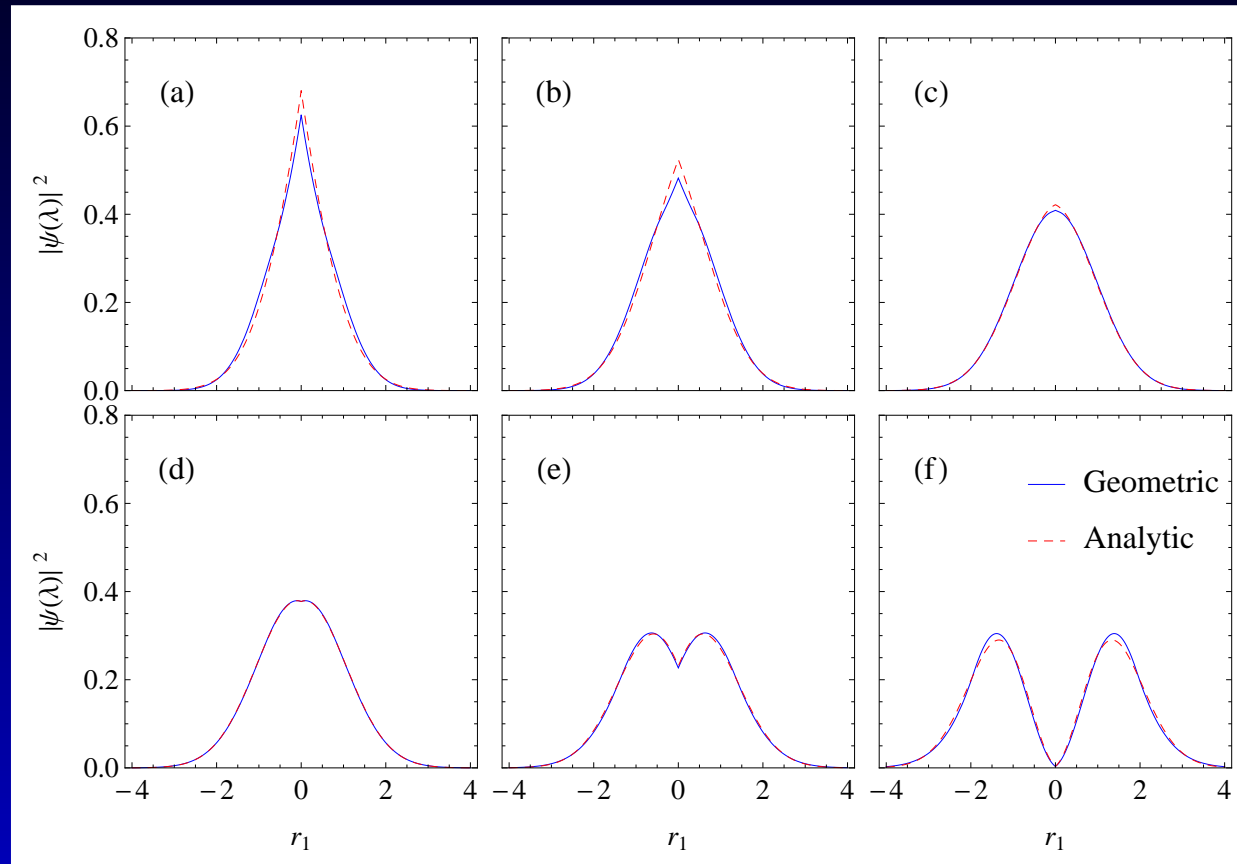
Ground state energies:
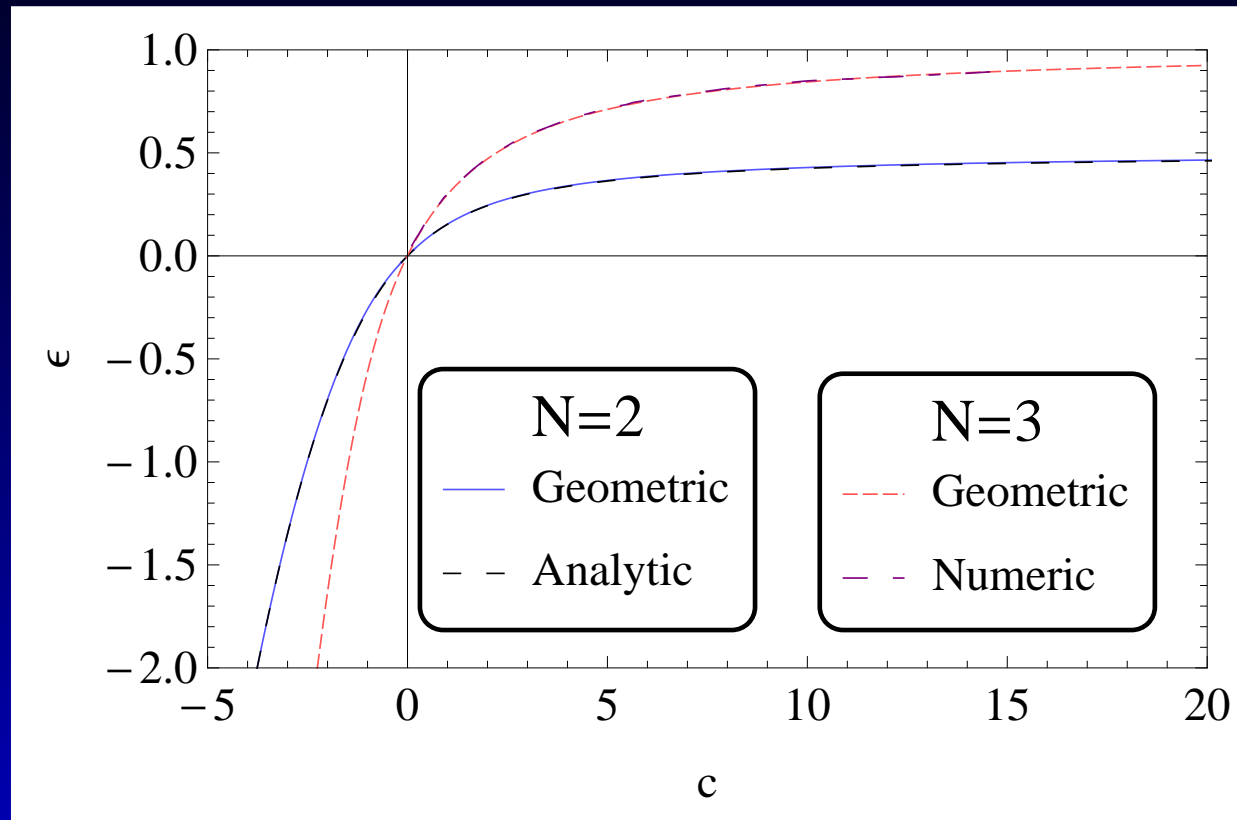
Ground state energies $\epsilon = \frac{En}{N\hbar\omega} - \frac{1}{2}$ as a function of the interaction strength c. The case $N = 2$ matches the analytic result well in all regimes and the $N = 3$ case matches numerical results.

D. Rubeni, A. Foerster and I. Roditi, PRA 2012

B. Wilson, A. Foerster, C. Kuhn, I. Roditi, D. Rubeni, PLA 2014

Probability density for $N = 2$:

Probability density $|\Psi|^2$ of the relative motion of two bosons in the GS for different values of the coupling: (a) $c = -1$, (b) $c = -0.5$, (c) $c = -0.1$, (d) $c = 0.1$, (e) $c = 1$ and (f) $c = 20$. In the attractive case it exhibits a peak at $r_1 = 0$ which increases and gets thinner for higher $|c|$ values, while for the repulsive case a cusp emerges at $r_1 = 0$ which goes to zero by increasing c

Probability density for $N = 3$:
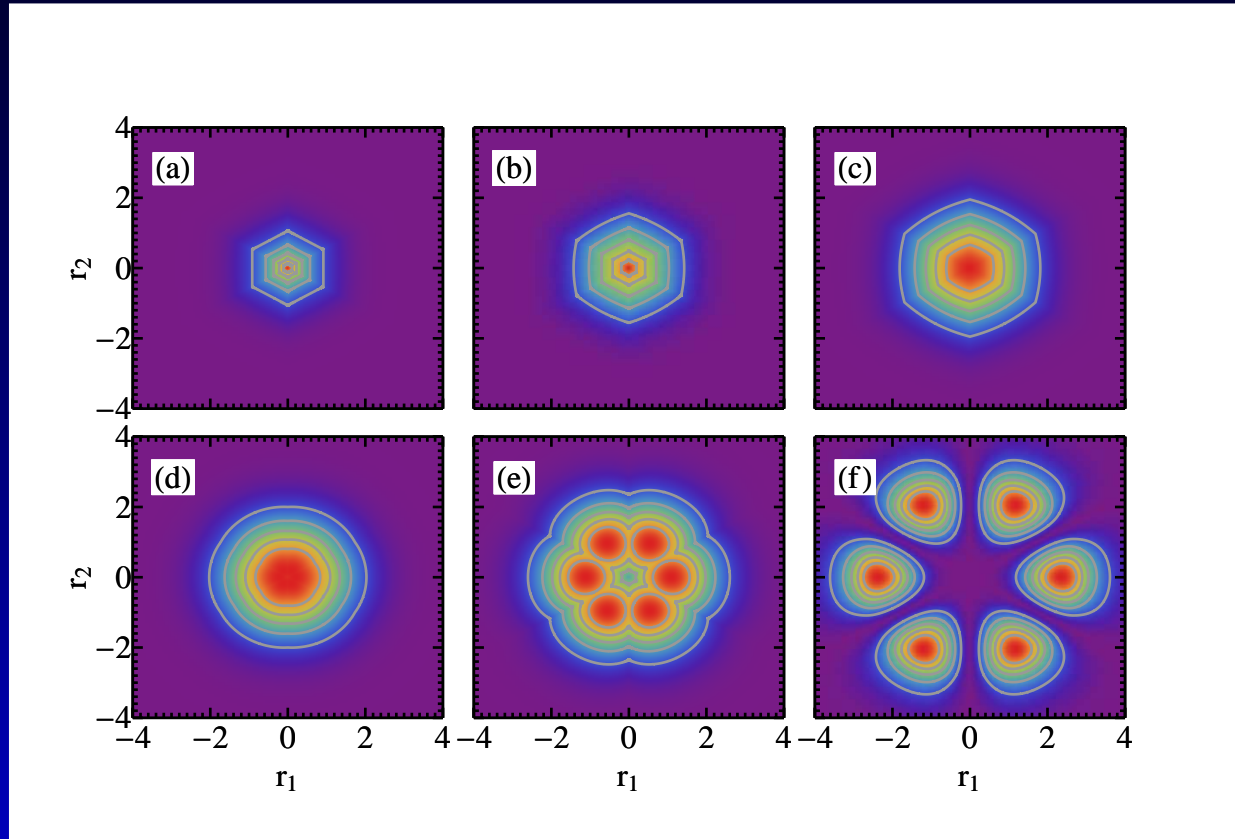
Probability density $|\Psi|^2$ in Jacobi coordinates r_1 and r_2 for different values of the coupling: (a) $c = -1$, (b) $c = -0.5$, (c) $c = -0.1$, (d) $c = 0.1$, (e) $c = 1$ and (f) $c = 20$.

The colors range from purple to red indicating respectively lower values and higher values of $|\Psi|^2$. In the attractive case a more localized peak is observed by increasing $|c|$. In the repulsive case $|\Psi|^2$ reduces along the mirror planes (the points where $x_i - x_j = 0$ when c increases.

Pair correlations:
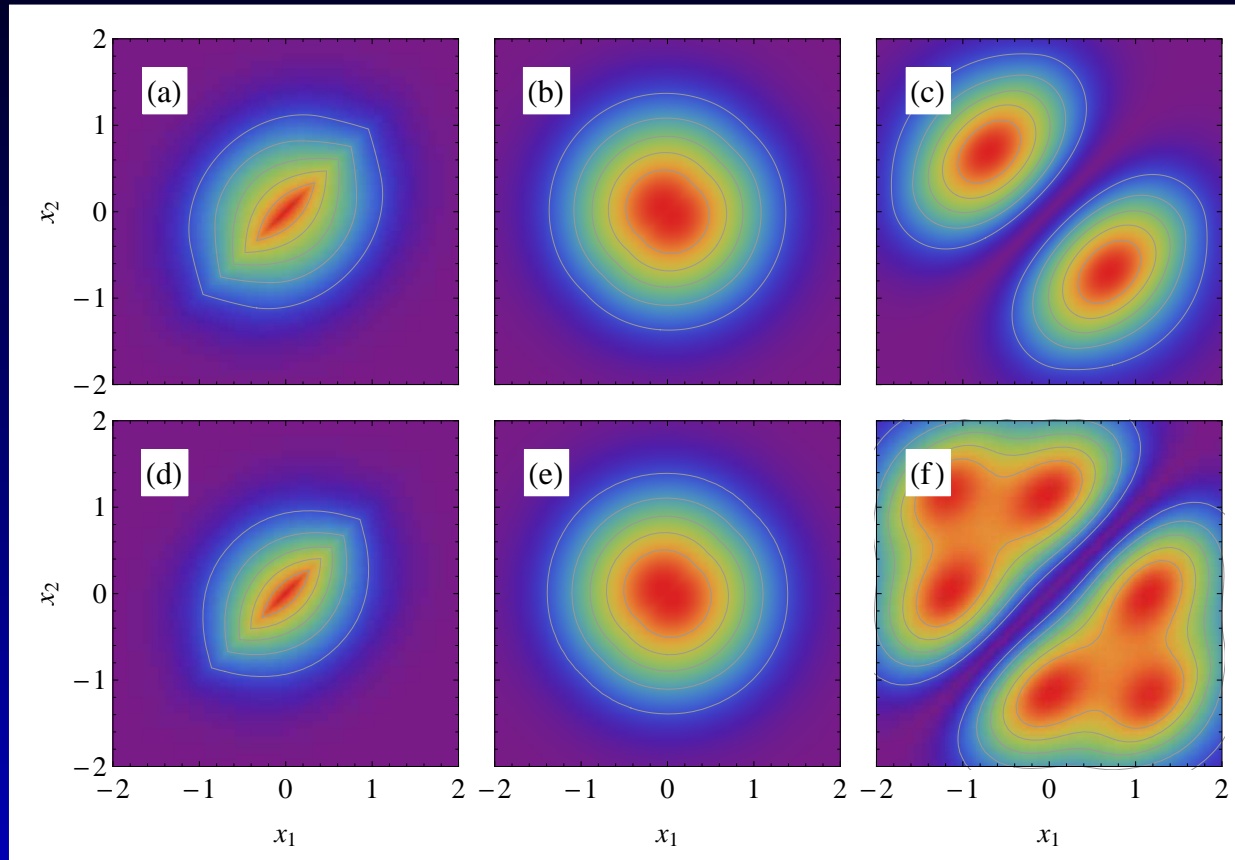
Pair correlation function $\rho_2(x_1, x_2)$ for $N = 2$ (upper line) for different values of the coupling:
(a) $c = -5$, (b) $c = 0.1$, (c) $c = 20$ and for $N = 3$ (bottom line) for: (d) $c = -5$, (e) $c = 0.1$
and (f) $c = 20$. In the repulsive case, the tendency of the particles to stay away from each other by
increasing c; in the attractive case the tendency of the particles to stay together by increasing $|c|$.

The BA+variational approach can be extended to higher N.

4- BREAKING THE INTEGRABILITY

Breakdown of the integrability: Heisenberg chain

Transport and control in one-dimensional systems

Lea F. Santos[1,a]

+ VIEW AFFILIATIONS

a) Electronic mail: lsantos2@yu.edu.

J. Math. Phys. **50**, 095211 (2009); http://dx.doi.org/10.1063/1.3181223

- The transport behavior in the integrable system contrasts with the non-integrable or chaotic chain, suggesting ballistic transport (integrable case) X diffusive transport (chaotic case).

- See also related work:
  M. Haque, D. Luitz, S. Mukerjee, H. Pastawski, R. Pereira, A. Polkovnikov, F. Pollmann, T. Prosen, J. Sirker

Breakdown of the integrability: Bose gas

$$H = -\frac{\hbar^2}{2m} \sum_{i=1}^{N} \frac{\partial^2}{\partial x_i^2} + \sum_{i<j\leq N} g_{ij}\delta(x_i - x_j)$$
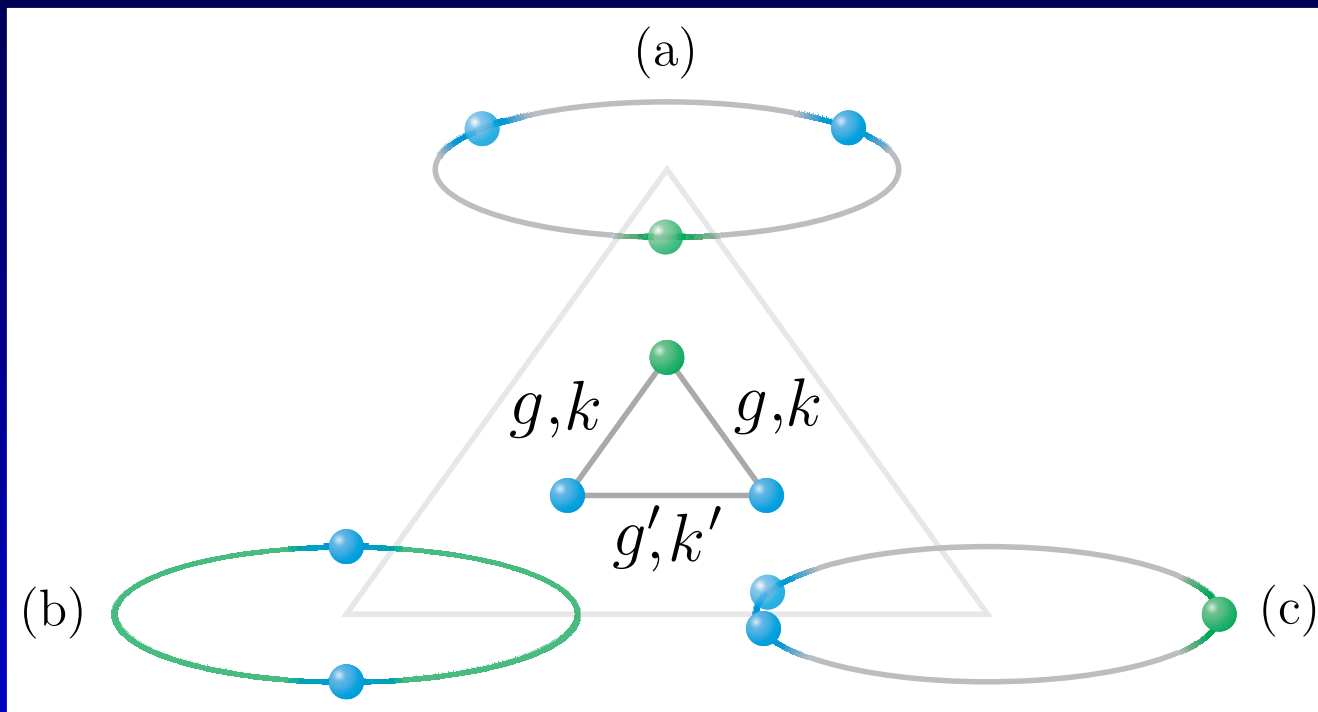
- N bosonic atoms of mass m in 1D;

- The interaction between each pair g_{ij} may differ.

- Here: repulsive case

- Jastrow-type Ansatz: Ψ_{ij} is the two-body exact solution

$$\Psi_J^v = C \prod_{i<j}^{P} (\Psi_{ij})^v$$

*Study the effect in static properties*

Simplest case: $N = 3$:

- $g_{12} = g_{13} = g, \quad g_{23} = g'$ (1: impurity, 2, 3: majority)

- Integrable case: $g = g'$.

Schematics for representative cases: (a) strongly repulsive integrable case, where separation between atoms is maximum (b) Interaction between majority pair is strong, impurity-majority interaction weak, so impurity appears delocalised across the ring (c) Impurity strongly repels majority pair but majority-majority interaction is weak, so these atoms tend to bunch together

Two-body density:
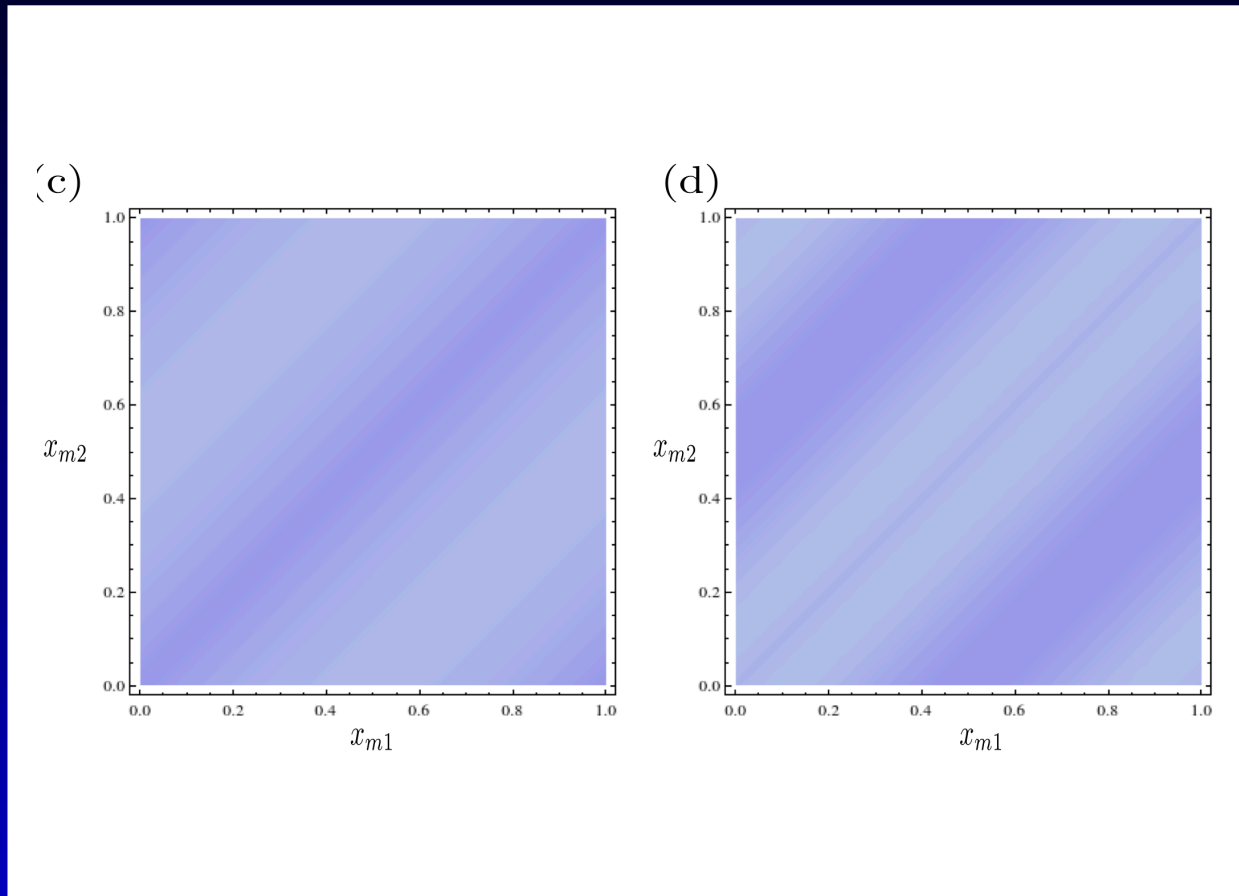
Two-body density for the majority pair for (c) integrable case and (d) non integrable case, where pronounced additional minima appear. The light (dark) color indicates high (low) density.

I. Brouzos and A. Foerster, PRA 2014

Breakdown of the integrability: Triple well

$$H = H_0 + b(N_2 - N_3)$$

$$
\begin{aligned}
H_0 &= U(N_1 + N_3 - N_2)^2 + \mu(N_1 + N_3 - N_2) \\
&+ t_1(a_1^\dagger a_2 + a_1 a_2^\dagger) + t_3(a_2^\dagger a_3 + a_2 a_3^\dagger)
\end{aligned}
\tag{3}
$$

- Integrable case: $b = 0$

  The model has 3 modes, so 3 independent conserved quantities are expected:

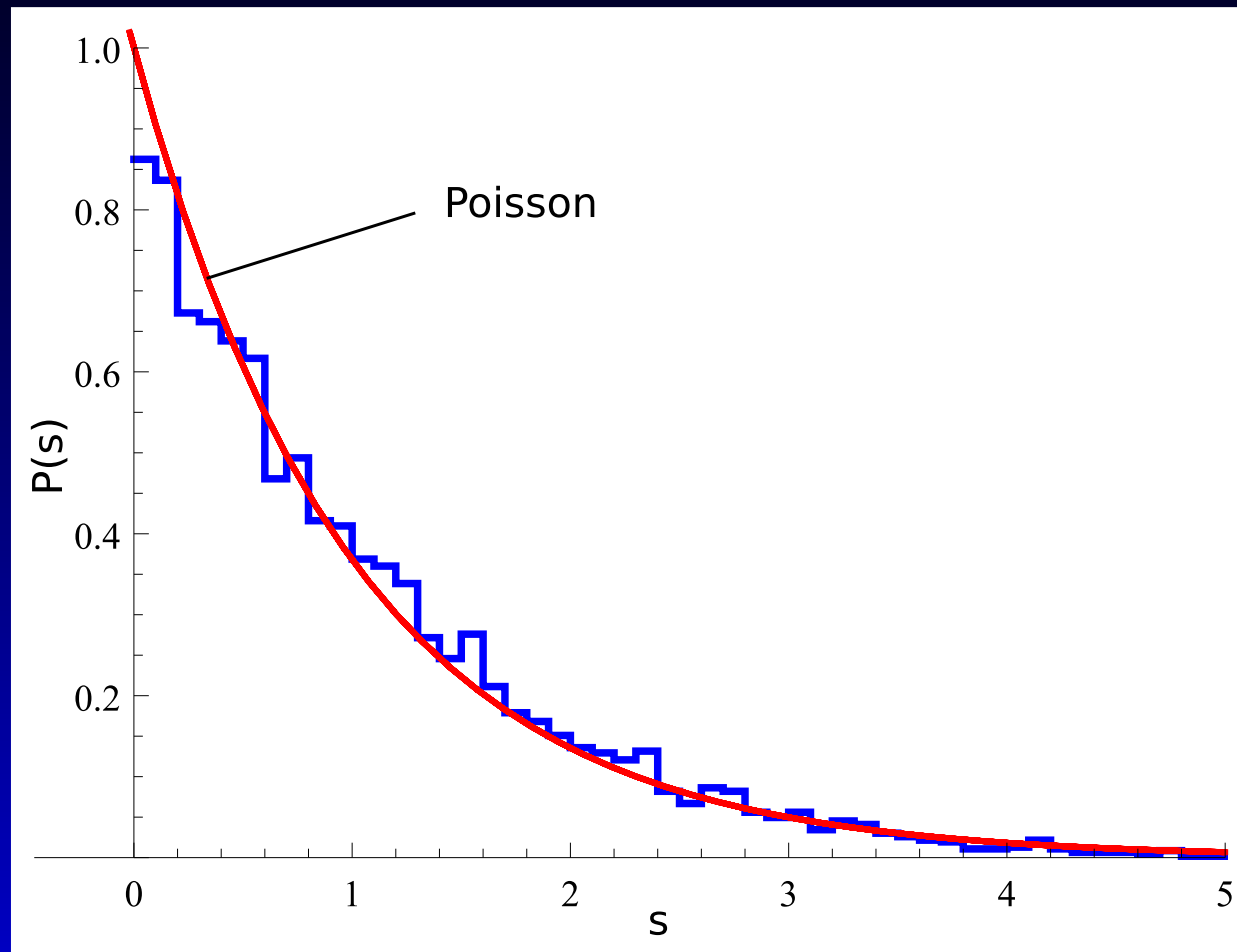$$[H_0, N] = [H_0, Q] = [N, Q] = 0$$

$$N = N_1 + N_2 + N_3 \quad Q = \frac{1}{t_1^2 + t_3^2}[t_1^2 N_3 + t_3^2 N_1 - t_1 t_3(a_3^\dagger a_1 + a_1^\dagger a_3)]$$

- Non-integrable case: $b \neq 0$

$$[H, N] = 0, \ [H, Q] \neq 0, \ [N, Q] \neq 0$$
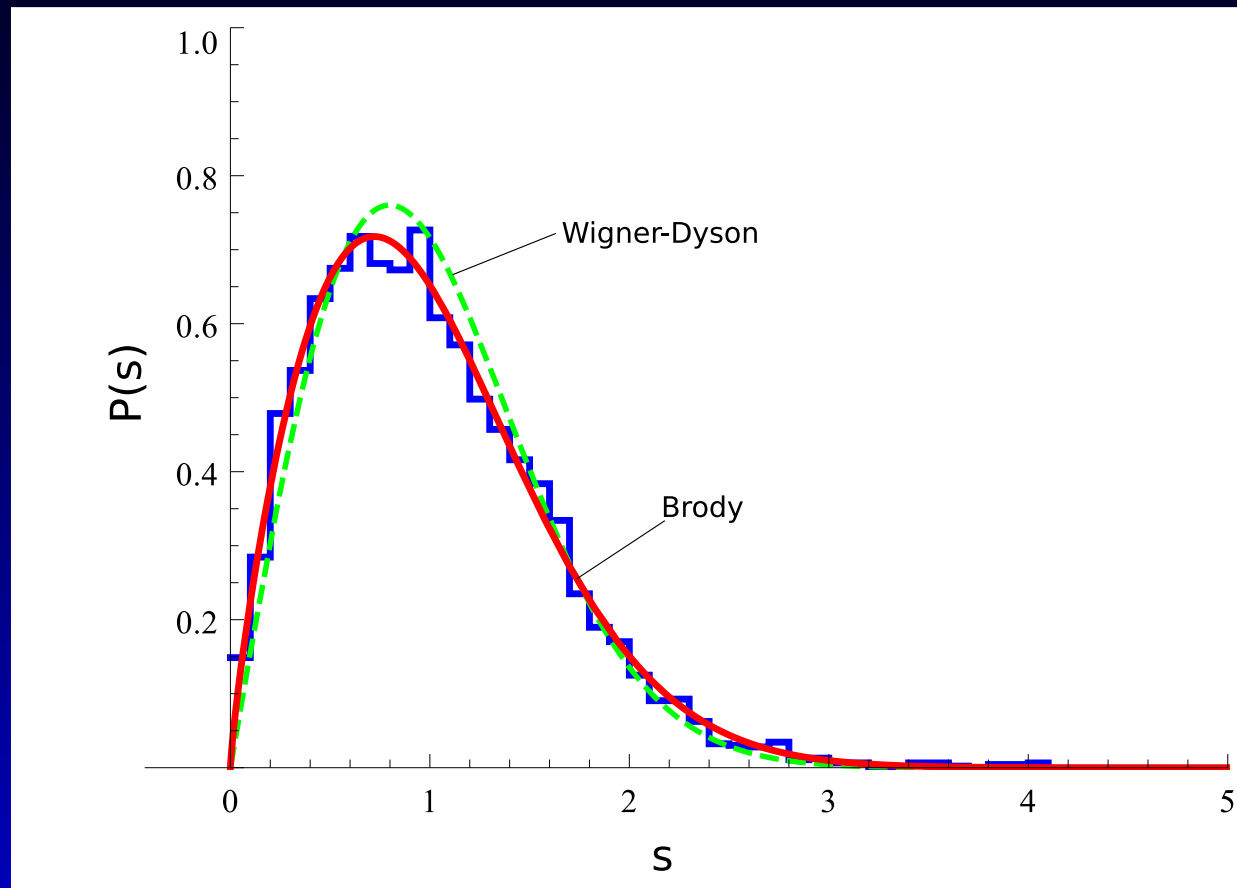
Level space distribution: *Integrable case* $b = 0$

Energy level spacing distribution as a function of the spacing "s".

$N = 100, \mu = 0, U = 1/100, t_1 = t_3 = 1/\sqrt{2}$. The distribution has universal behaviour

independent of the choice of coupling parameters and follows the Poisson distribution

$$P(s) = \exp(-s) \text{ (red curve)}$$

Level space distribution: *Non-integrable case $b \neq 0$*

Energy level spacing distribution as a function of the spacing "s".

$N = 100, \mu = 0, U = 1/100, t_1 = t_3 = 1/\sqrt{2}, b = 1$. The distribution follows the Brody

distribution (red curve), very close to the Wigner-Dyson distribution (green curve).

$$P_W(s) = \frac{\pi s}{2} \exp(-\frac{\pi s^2}{4}); \quad P_{B(s)} = \alpha(q+1)s^q \exp(-\alpha s^{q+1}); \quad \alpha = \left[\Gamma\left(\frac{q+2}{q+1}\right)\right]^{q+1}$$

5- CONCLUDING REMARKS

Concluding remarks:

- We have presented some examples in which integrable models are relevant. This list should be considered remarkable, not necessarily because of the examples given, but arguably also because of what has been omitted.

- There are a wealth of integrable models which are yet to find their way into experiments.

- It is clear that integrable models will continue to offer valuable insights into the description of physical properties and experimental results for decades to come.

Collaborators

1. Prof. Murray T. Batchelor, ANU-Australia

2. Prof. Jon Links, UQ-QLD-Australia

3. Prof. Xi-Wen Guan, Wuhan-China

4. * Prof. Ivan S. Oliveira, CBPF-Brazil

5. Prof. Itzhak Roditi, CBPF-Brazil

6. Prof. Arlei Tonel, Unipampa-Brazil

7. Prof. Leandro Yimai, Unipampa-Brazil

8. Prof. Nikolaj T. Zinner, Aarhus University, Denmark

9. Dr. Ioannis Brouzos

10. Dr. Carlos Kuhn, ANU-Australia

11. Dr. Diefferson Lima, UQ-QLD-Australia

12. Dr. Brendan Wilson, ANU-Australia

13. * Dr. Fatima Anvari, (post-doc), UFRGS-Brazil

14. Rafael Barfknecht (PHd student), UFRGS-Brazil

15. David Carvalho (PHd student), UFRGS-Brazil

16. Karin Wilsmann (Master student), UFRGS-Brazil

Thank you for your attention

Integrability: Formal definition

It is generally accepted that an integrable system is one which is derived from a set of commuting transfer matrices.

This definition applies to many-body systems.

Transfer matrix $\tau(u)$: is a generating function of conserved quantities

- The condition:

$$[\tau(u), \tau(v)] = 0$$

- represents (an infinite set of) conservation laws:

$$[c_n, c_m] = 0$$

- where the series expansion was taken:

$$\tau = \sum_n c_n v^n$$

Integrability: In practice

Means that we can solve the eigenvalue problem of the transfer matrix and consequently the hamiltonian derived from it.

Method: Bethe ansatz

- Problem: Find the spectrum of τ:
  $$\tau\Psi = E\Psi \ (1)$$

- Ansatz:
  $$\Psi = B(v_1)B(v_2)\ldots B(v_N)\Phi \ (2)$$

- Substituting (2) in (1): $\tau\Psi = E\Psi + u.t.(\{v_i\})$

- The condition of the cancelation of the unwanted terms implies in a set of conditions for the v_i, called BAE.

- This will ensure that Ψ will be the eigenvector of τ with energy E.

Integrability:

- ## Classical Mechanics

  If a system with n degrees of freedom possesses n independent first integrals of motion in involution (i.e. Poisson-commuting), then the system is integrable (Liouville)

- ## Quantum Mechanics: Common definitions

  - 1) A system is quantum integrable if it possesses a maximal set of independent commuting quantum operators $Q_\alpha, \alpha = 1, \ldots dim(H)$.

  - 2) A system is quantum integrable if it is exactly solvable, in other words if we can construct its full set of eigenstates explicitly.

  - 3) A system is quantum integrable if it can be mapped to harmonic oscillators.

  - 4) A system is quantum integrable if the scattering it supports is nondiffractive.

  - 5) A system is quantum integrable if its energy level statistics is Poissonian.

  - 6) A system is quantum integrable if it shows level crossings (i.e. does not show level repulsion).

Two-body density or pair correlations:

$$\rho_2(x_1, x_2) = \int_{-\infty}^{+\infty} \ldots \int_{-\infty}^{+\infty} |\Psi|^2 dx_3 \ldots dx_N$$

It gives the probability of finding 2 particles at 2 given positions at the same time.

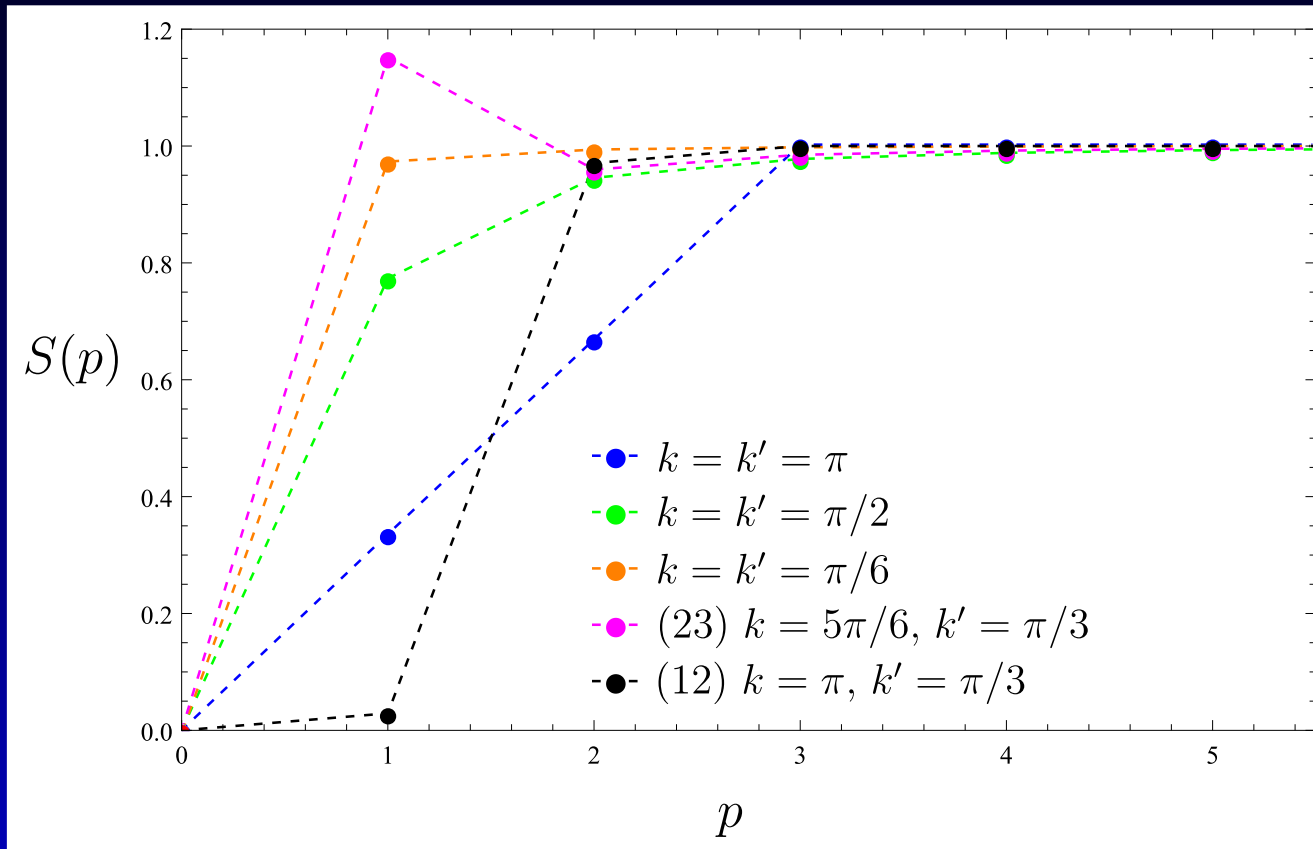- The two-body density of the majority pair of atoms:

$$\rho(x_{m_1}, x_{m_2}) = \frac{\int |\psi|^2 dx_i}{\int |\psi|^2 dx_i dx_{m_1} dx_{m_2}}$$

- Jacobi coordinates:

$$\xi = \frac{2}{3}\left(x_i - \frac{x_{m_1} + x_{m_2}}{2}\right), \ r = x_{m_1} - x_{m_2}$$

The ξ Jacobi coordinate represents the position of the impurity, depending on the position of the center of mass of the majority atoms.

Static structure factor:

Static structure factor S as a function of momentum p for different values of interactions in the integrable and non-integrable cases. For high p, S converges to 1. For low p, S of the majority atoms exhibits a peak for strong majority-impurity repulsion, attributed to an effective attraction.

R. Barfknecht, I. Brouzos and A. Foerster, PRA 2015

Fermi gas: Bethe ansatz method

C.N. Yang, PRL **19***(1967)1312; M. Gaudin, Phys. Lett.* **24** *(1967) 55*

- Energy:
$$E = \frac{\hbar^2}{2m} \sum_{j=1}^{N} k_j^2,$$

- BAE:

$$\exp(\mathrm{i}k_j L) = \prod_{\ell=1}^{M} \frac{k_j - \Lambda_\ell + \mathrm{i}\,c/2}{k_j - \Lambda_\ell - \mathrm{i}\,c/2}$$

$$\prod_{\ell=1}^{N} \frac{\Lambda_\alpha - k_\ell + \mathrm{i}\,c/2}{\Lambda_\alpha - k_\ell - \mathrm{i}\,c/2} = -\prod_{\beta=1}^{M} \frac{\Lambda_\alpha - \Lambda_\beta + \mathrm{i}\,c}{\Lambda_\alpha - \Lambda_\beta - \mathrm{i}\,c}$$

$\{k_j,\, j=1,\dots,N\}$ are the quasimomenta for the fermions;

$\{\Lambda_\alpha,\, \alpha=1,\dots,M\}$ are the rapidities for the internal spin degrees of freedom

The solutions to the BAE give the GS properties and provide a clear pairing signature

Thermodynamical Bethe Ansatz - TBA

- elegant method to study thermodynamical properties

- thermodynamic limit: $L \to \infty$, $N \to \infty$ with N/L finite:

  - consider a distribution function for the BA-roots;

  - the equilibrium state is determined by the condition of minimizing the Gibbs free energy:
  $$G = E - HM^z - \mu N - TS$$

- the TBA equations are a set of coupled nonlinear equations from which we can obtain the phase diagram at $T = 0$ for strong and weak coupling.

TBA - equations:

set of coupled nonlinear integral equations

$$\epsilon^{\mathrm{b}}(k) \;=\; 2(k^2 - \mu - \frac{1}{4}c^2) + Ta_2 * \ln(1 + \mathrm{e}^{-\epsilon^{\mathrm{b}}(k)/T})$$

$$+ Ta_1 * \ln(1 + \mathrm{e}^{-\epsilon^{\mathrm{u}}(k)/T})$$

$$\epsilon^{\mathrm{u}}(k) \;=\; k^2 - \mu - \frac{1}{2}H + Ta_1 * \ln(1 + \mathrm{e}^{-\epsilon^{\mathrm{b}}(k)/T})$$

$$- T\sum_{n=1}^{\infty} a_n * \ln(1 + \eta_n^{-1}(k))$$

$$\ln \eta_n(\lambda) \;=\; \frac{nH}{T} + a_n * \ln(1 + \mathrm{e}^{-\epsilon^{\mathrm{u}}(\lambda)/T})$$

$$+ \sum_{n=1}^{\infty} T_{nm} * \ln(1 + \eta_m^{-1}(\lambda))$$

in terms of the dressed energies: $\epsilon^{\mathrm{b}}(k)$ and $\epsilon^{\mathrm{u}}(k)$ for paired and unpaired fermions and the function $\eta_n(\lambda)$. The Gibbs free energy per unit length is:

$$G = -\frac{T}{\pi} \int_{-\infty}^{\infty} dk \ln(1 + \mathrm{e}^{-\epsilon^{\mathrm{b}}(k)/T}) - \frac{T}{2\pi} \int_{-\infty}^{\infty} dk \ln(1 + \mathrm{e}^{-\epsilon^{\mathrm{u}}(k)/T})$$

Limit $T \to 0$: dressed energy equations

$$\epsilon^{\mathrm{b}}(\Lambda) = \qquad 2(\Lambda^2 - \mu - \frac{c^2}{4}) - \int_{-B}^{B} a_2(\Lambda - \Lambda')\epsilon^{\mathrm{b}}(\Lambda')d\Lambda'$$

$$- \int_{-Q}^{Q} a_1(\Lambda - k)\epsilon^{\mathrm{u}}(k)dk$$

$$\epsilon^{\mathrm{u}}(k) = \qquad (k^2 - \mu - \frac{H}{2}) - \int_{-B}^{B} a_1(k - \Lambda)\epsilon^{\mathrm{b}}(\Lambda)d\Lambda$$

$$a_m(x) = \frac{1}{2\pi} \frac{m|c|}{(m\,c/2)^2 + x^2}, \;\; \epsilon^{\mathrm{b}}(\pm B) = \epsilon^{\mathrm{u}}(\pm Q) = 0$$

The Gibbs free energy per unit length at zero temperature is given by

$$G(\mu, H) = \frac{1}{\pi} \int_{-B}^{B} \epsilon^{\mathrm{b}}(\Lambda)d\Lambda + \frac{1}{2\pi} \int_{-\mathbf{Q}}^{\mathbf{Q}} \epsilon^{\mathrm{u}}(\mathbf{k})\mathbf{dk}$$

From the Gibbs free energy per unit length we have the relations

$$-\partial G(\mu, H)/\partial \mu = n, \;\; -\partial G(\mu, H)/\partial H = m_z = nP/2$$

Strong attraction

$$H \;=\; \frac{\hbar^2 n^2}{2m}\left\{ \frac{\gamma^2}{2} + 2P^2\pi^2 \left(1 + \frac{4(1-P)}{|\gamma|} - \frac{4P}{3|\gamma|} \right) \right.$$
$$\left. - \frac{\pi^2(1-P)^2}{8} \left(1 + \frac{4P}{|\gamma|} \right) \right\}.$$

CRITICAL FIELDS:

$$H_{c1} \;=\; \frac{\hbar^2 n^2}{2m}\left(\frac{\gamma^2}{2} - \frac{\pi^2}{8} \right)$$

$$H_{c2} \;=\; \frac{\hbar^2 n^2}{2m}\left[\frac{\gamma^2}{2} + 2\pi^2 \left(1 - \frac{4}{3|\gamma|} \right) \right]$$

Direct verification of the YBE using NMR:

OPEN | **Experimental realization of the Yang-Baxter Equation via NMR interferometry**

F. Anvari Vind[1,2], A. Foerster[2], I. S. Oliveira[1], R. S. Sarthour[1], D. O. Soares-Pinto[3], A. M. Souza[1] & I. Roditi[1]

The Yang-Baxter equation is an important tool in theoretical physics, with many applications in different domains that span from condensed matter to string theory. Recently, the interest on the equation has increased due to its connection to quantum information processing. It has been shown that the Yang-Baxter equation is closely related to quantum entanglement and quantum computation. Therefore, owing to the broad relevance of this equation, besides theoretical studies, it also became significant to pursue its experimental implementation. Here, we show an experimental realization of the Yang-Baxter equation and verify its validity through a Nuclear Magnetic Resonance (NMR) interferometric setup. Our experiment was performed on a liquid state Iodotrifluoroethylene sample which contains molecules with three qubits. We use Controlled-transfer gates that allow us to build a pseudo-pure state from which we are able to apply a quantum information protocol that implements the Yang-Baxter equation.

based on a proposal by Mo-Lin Ge et al, PRA 2008

Optical simulation of the Yang-Baxter equation

Shuang-Wei Hu,[1] Kang Xue,[2] and Mo-Lin Ge[1,*]
[1]*Theoretical Physics Division, Chern Institute of Mathematics, Nankai University, Tianjin 300071, People's Republic of China*
[2]*Department of Physics, Northeast Normal University, Changchun, Jilin 130024, People's Republic of China*

In this paper, several proposals of optically simulating Yang-Baxter equations have been presented. Motivated by the recent development of anyon theory, we apply Temperley-Lieb algebra as a bridge to recast a four-dimensional Yang-Baxter equation into its two-dimensional counterpart. In accordance with both representations, we find the corresponding linear-optical simulations, based on the highly efficient optical elements. Both the degrees of freedom of photon polarization and location are utilized as the qubit basis, in which the unitary Yang-Baxter matrices are decomposed into a combination of actions of basic optical elements.

Direct verification of the YBE through an NMR setup

- Our experiment is performed on a liquid state Iodotrifluoroethylene (C_2F_3I) sample which contains molecules with three qubits.

  F1, F2 and F3 are denoted as qubit 1, qubit 2 and qubit 3, respectively.

  Quantum circuit diagram for implementation of the YBE.

- LHS and RHS of the YBE are applied on qubits 1 and 3, respectively. The YBE can be reduced to a sequence of single spin rotations, which is the sequence implemented in the experiment. The qubits 1 and 3 are left in the output states Φ_1 and Φ_3, respectively. To verify the YBE we need to measure the overlap , if this quantity is equal to 1, then the YBE is satisfied, otherwise the YBE is not satisfied.
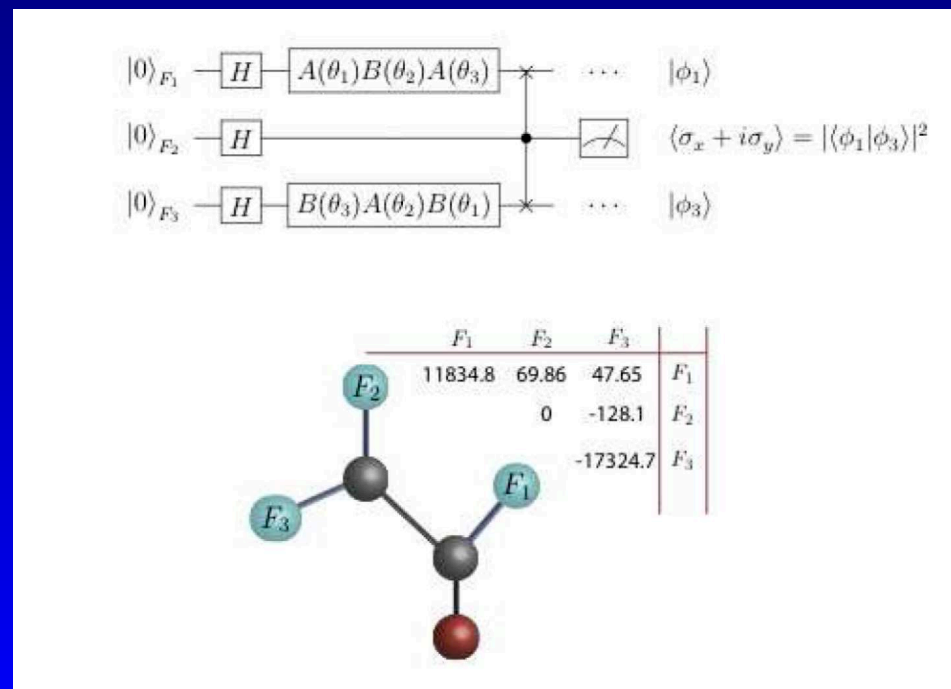
Direct verification of the YBE using quantum optics:

Direct experimental simulation of the Yang–Baxter equation

Chao Zheng,[1,2] Jun-lin Li,[1] Si-yu Song,[1] and Gui Lu Long[1,2,*]

[1]State Key Laboratory of Low-Dimensional Quantum Physics and Department of Physics, Tsinghua University, Beijing 100084, China
[2]Tsinghua National Laboratory for Information Science and Technology, Beijing 100084, China
*Corresponding author: gllong@tsinghua.edu.cn

Having been introduced in the field of many bodies of statistical mechanics, the Yang–Baxter equation has become an important tool in a variety of fields of physics. In this work, we report the first direct experimental simulation of the Yang–Baxter equation using linear quantum optics. The equality between the two sides of the Yang–Baxter equation in two dimension has been demonstrated directly, and the spectral parameter transformation in the Yang–Baxter equation is explicitly confirmed. © 2013 Optical Society of America
OCIS codes: (030.0030) Coherence and statistical optics; (270.0270) Quantum optics.
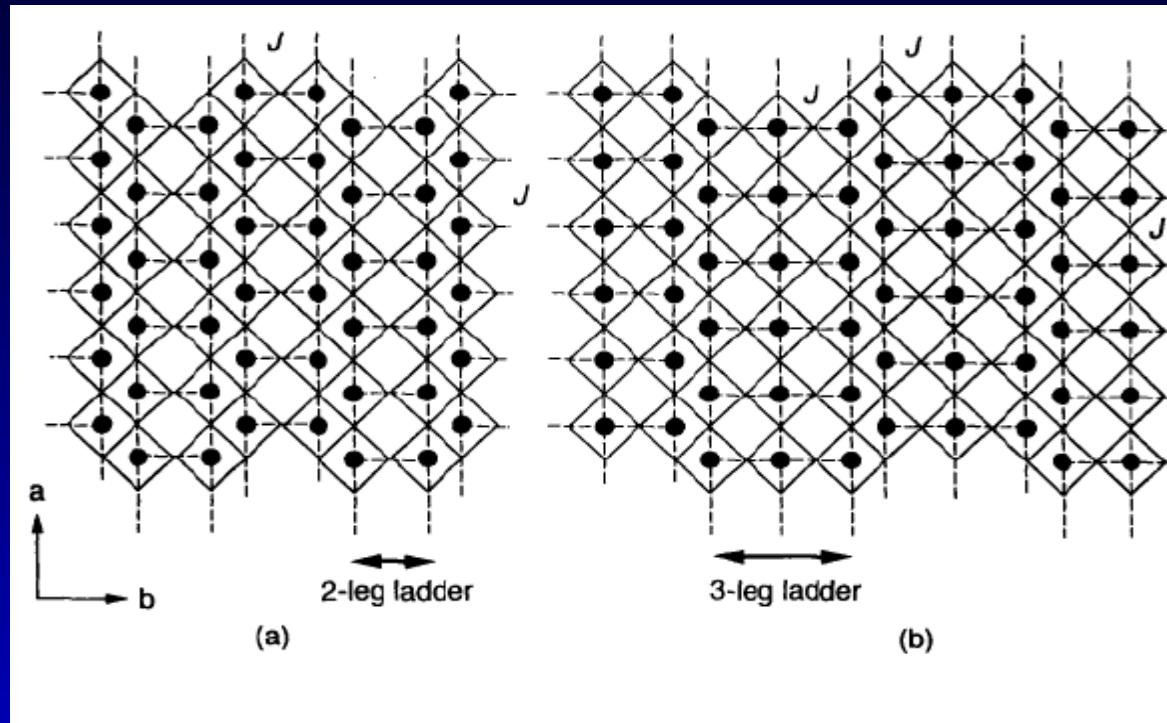http://dx.doi.org/10.1364/JOSAB.30.001688

$$A(u) = \begin{pmatrix} e^{-i\theta} & 0 \\ 0 & e^{i\theta} \end{pmatrix} \equiv A(\theta)$$

$$B(u) = \begin{pmatrix} \cos\theta & -i\,\sin\theta \\ -i\,\sin\theta & \cos\theta \end{pmatrix} \equiv B(\theta)$$

$$A(\theta_1)\, B(\theta_2)\, A(\theta_3) = B(\theta_3) A(\theta_2) B(\theta_1)$$

$$\tan(\theta_2) = \frac{\sin(\theta_1 + \theta_3)}{\cos(\theta_1 - \theta_3)}$$
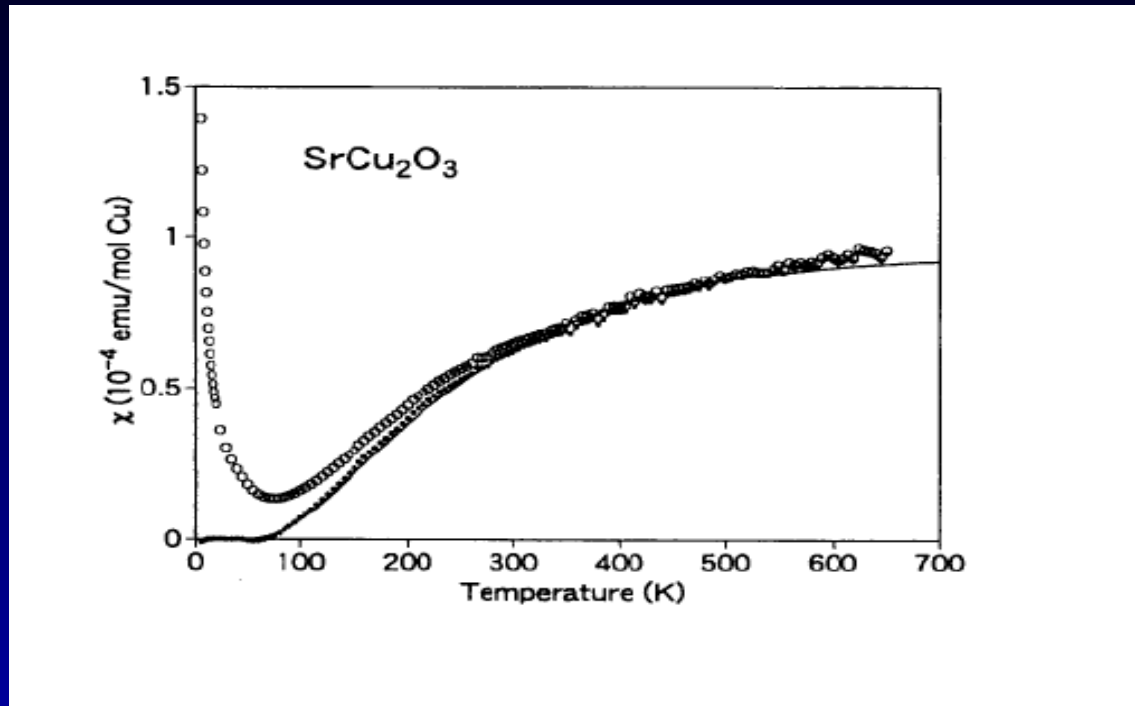
SPIN LADDER: Schematic Representation:

$$L\text{=}2: SrCu_2O_3 \qquad L = 3 : Sr_2Cu_3O_5$$

Azuma et al, PRL 94

- Cooper: represented by points, Oxigens: located at the corners

- Intra-ladder coupling is weak
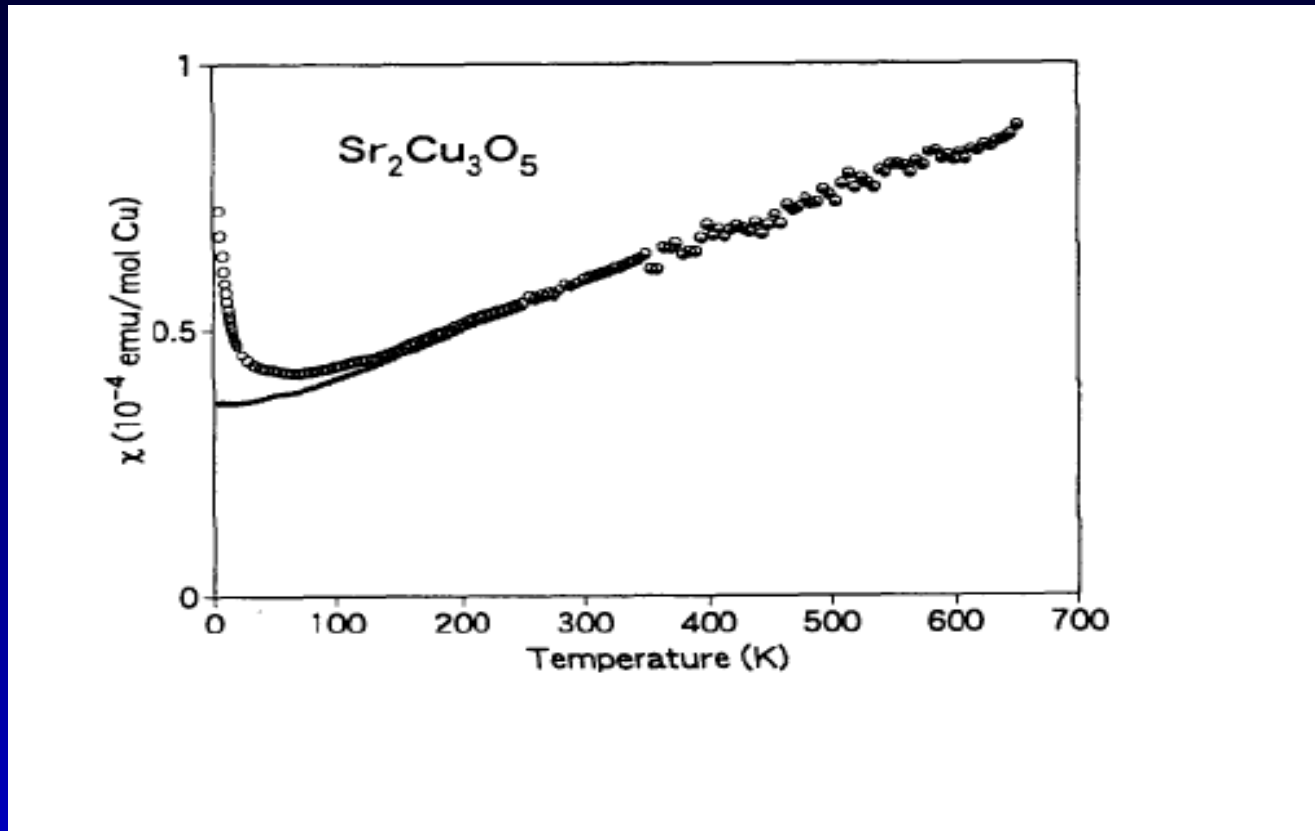
2-leg ladder: Susceptibility X T

Shows an exponential decay: (from which we get the gap)

$$\chi = C\frac{e^{-\frac{\Delta}{T}}}{\sqrt{T}};\ T \to 0$$

Troyer et al, PRL54 (1996); Azuma et al, PRL73 (1994)

3-leg ladder: Susceptibility X T

There is NO exponential decay: (There is no gap)

$\chi(T)$ *tends to a finite number as* $T \to 0$

Troyer et al, PRL54 (1996); Azuma et al, PRL73 (1994)

SPIN LADDER: QTM and HTE:

Table 1. Comparison between the experimental values for the critical points H_{c1} and H_{c2} for strong coupling ladder compounds and the TBA results obtained from the $su(4)$ integrable model.

Compounds	g	$J_\perp$ (K)	$J_\parallel$ (K)	γ	H_{c1} (exp) (T)	H_{c2} (exp) (T)	H_{c1} (TBA) (T)	H_{c2} (TBA) (T)
B5i2aT	2.1	13	1.15	4	8.4	10.4	8.3	10.03
Cu(Hp)Cl	2.03	13.2	2.5	4	7.5	13.2	7.84	11.51
BPCB	2.13	13.3	3.8	4	6.6	14.6	6.6	11.95
KCuCl$_3$	2.05	49.2	12.3	2.68	22.4	≈60	22.4	49

We demonstrate here that the integrable $su(4)$ ladder model [3,4] is capable of describing the physics of the ladder compounds. Indeed, the thermodynamic Bethe ansatz (TBA) applied to the integrable $su(4)$ ladder model predicts the critical fields $H_{c1} = J_\perp - 4J_\parallel/\gamma$ and $\mu_B g H_{c2} = J_\perp + 4J_\parallel/\gamma$, where γ is a rescaling parameter, which are also good fits for the strong coupling compounds [5]. Very recently the high temperature expansion (HTE) method [6,7] suggested

where $\vec{S}_j$ and $\vec{T}_j$ are Heisenberg operators, μ_B is the Bohr magneton, and g is the Landé factor. Throughout, L is the number of rungs and periodic boundary conditions are imposed. In the strong coupling limit, the contribution to the low-temperature physics from the multibody term in $\mathcal{H}_{\text{leg}}$ is minimal and, as a consequence, the integrable ladder Hamiltonian exhibits similar critical behavior to the standard Heisenberg ladder [5]. We adapt the model into the QTM method [9]. The eigenvalue of the QTM (up to a constant) is obtained by the nested Bethe ansatz to be

$$T_1^{(1)}(v, v_i^{(a)}) = e^{\beta\mu_1}\phi_-(v - i)\phi_+(v)\frac{Q_1(v + \frac{1}{2}i)}{Q_1(v - \frac{1}{2}i)} + e^{\beta\mu_2}\phi_-(v)\phi_+(v)\frac{Q_1(v - \frac{3}{2}i)Q_2(v)}{Q_1(v - \frac{1}{2}i)Q_2(v - i)}$$

$$+ e^{\beta\mu_3}\phi_-(v)\phi_+(v)\frac{Q_2(v - 2i)Q_3(v - \frac{1}{2}i)}{Q_2(v - i)Q_3(v - \frac{3}{2}i)} + e^{\beta\mu_4}\phi_-(v)\phi_+(v + i)\frac{Q_3(v - \frac{5}{2}i)}{Q_3(v - \frac{3}{2}i)}. \tag{2}$$

In this equation the chemical potential terms are $\mu_1 = J_\perp/2$, $\mu_2 = \mu_B g H$, $\mu_3 = 0$, and $\mu_4 = -\mu_B g H$, with $\phi_\pm(v) = (v \pm iu_N)^{N/2}$. The inhomogeneity parameter $u_N = -(J_\parallel\beta/\gamma N)$, with $Q_a[v] = \prod_{i=1}^{M^{(a)}}(v - v_i^{(a)})$, for $a = 1, 2, 3$. Here N denotes the Trotter-Suzuki number. The fused $T_m^{(a)}$ system [8], which denotes the row-to-row transfer matrix with fusion type (a, m) in the auxiliary space carrying the m-fold symmetric tensor of the ath fundamental representation of the

SPIN LADDER: QTM and HTE:

$su(4)$ algebra, is essentially generated by the QTM eigenvalue $T_1^{(1)}$ in (2). Thus $T_1^{(1)}$ can be embedded into the fused $T_m^{(a)}$ system. The analytic nonzero and constant asymptotic properties of the normalized $\tilde{T}_m^{(a)}(v)$ system suggest the expansion ansatz

$$\lim_{N\to\infty} \tilde{T}_1^{(a)}(v) = \exp\left[\sum_{n=0}^{\infty} b_n^{(a)}(v)\left(\frac{J_\parallel}{\gamma T}\right)^n\right], \tag{3}$$

with $b_n^{(a)}(v) = \sum_{j=0}^{n-1} c_{n,j}^{(a)} v^{2j}/[v^2 + (a+1)^2/4]^n$. The QTM eigenvalue satisfies a set of the nonlinear integral equations [7]

$$\tilde{T}_1^{(a)}(v) = Q_1^{(a)} + \oint_{C_m^{(a)}} \frac{dy}{2\pi i} \frac{1}{v - y - \beta_1^{(a)}}\left[\frac{\tilde{T}_1^{(a-1)}(y + \beta_1^{(a)} - \frac{1}{2}i)\tilde{T}_1^{(a+1)}(y + \beta_1^{(a)} - i)}{\tilde{T}_1^{(a)}(y + \beta_1^{(a)} - i)}\right]$$

$$+ \oint_{\bar{C}_m^{(a)}} \frac{dy}{2\pi i} \frac{1}{v - y + \beta_1^{(a)}}\left[\frac{\tilde{T}_1^{(a-1)}(y - \beta_1^{(a)} + \frac{1}{2}i)\tilde{T}_1^{(a+1)}(y - \beta_1^{(a)} + \frac{1}{2}i)}{\tilde{T}_1^{(a)}(y - \beta_1^{(a)} + i)}\right], \quad a = 1, 2, 3. \tag{4}$$

Following Ref. [7], the coefficients $c_{n,j}^{(a)}$ can be obtained recursively from Eq. (4) with initial conditions $b_0^{(a)} = \ln Q_1^{(a)}$, where $Q_1^{(a)}$ are constants related to the chemical potential terms via $\lim_{N\to\infty}\lim_{|v|\to\infty}\tilde{T}_1^{(a)}(v) = Q_1^{(a)}$ with $Q_1^{(0)} = 1$ and $Q_1^{(4)} = \exp(J_\perp/2T)$. In this way the spin ladder free energy $f(T,H) = -T\ln T_1^{(1)}$ can be expanded in powers of $J_\parallel/\gamma T$. For the first few orders we have

$$-\frac{1}{T}f(T,H) = \ln(2B_{\epsilon,1}) + A\left(\frac{J_\parallel}{\gamma T}\right)$$

$$+ \frac{3}{2}\left(A - A^2 + \frac{1}{2}\frac{\epsilon B_{1,\epsilon}}{B_{\epsilon,1}^3}\right)\left(\frac{J_\parallel}{\gamma T}\right)^2, \tag{5}$$

where $A = B_{\epsilon,0}(1 + 2B_{0,1})/B_{\epsilon,1}^2$ with $\epsilon = \exp(J_\perp/2T)$ and

$$B_{x,y} = x\cosh\left(\frac{J_\perp}{2T}\right) + y\cosh\left(\frac{\mu_B gH}{T}\right). \tag{6}$$

We find that the analytic expression (5) is sufficiently accurate to evaluate the model's thermodynamics. Nevertheless, we have considered the HTE up to fifth order.

The theoretical curves for the high field magnetization shown in Fig. 2 for different temperatures are also in good agreement with the experimental values. The field dependent magnetization curve predicts the low-temperature phase diagram as well as the magnetization plateaus. For very low temperature the rung singlet forms a dimerized ground state if the magnetic field is below the critical field H_{c1}. The length of the antiferromagnetic correlation is finite while the triplet state is gap full. For finite temperatures the triplet excitations are also involved in the gapped phase. This can be observed in the high field magnetization curves for $T = 1.59$ K and $T = 4.35$ K in Fig. 2. At the critical field H_{c1}, the gap is closed with $\mu_B gH_{c1} = \Delta$. If the magnetic field is above the critical point H_{c1}, the lower triplet component becomes
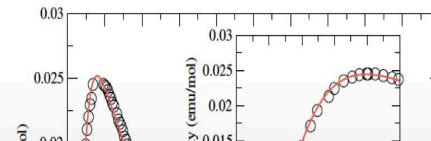
SPIN LADDER: THERMODYNAMICAL PROPERTIES

- The thermal and magnetic properties can be obtained by exact diagonalization or by analytical methods: the free energy is written in terms of the eigenvalue of the Quantum Transfer Matrix (QTM) (the QTM eigenvalue satisfies a set on nonlinear eqs. The free energy can be expanded in powers of $J_{\parallel}/(\gamma T)$ up to fifth order, using the High Temperature Expansion - HTE), and from it we derive the thermodynamical properties by standard thermodynamics:

- *Magnetization*

$$M_z = -\frac{\partial}{\partial H} f(T, H)$$

- *Magnetic susceptibility*

$$\chi = -\frac{\partial^2}{\partial H^2} f(T, H)$$

- *Specific heat*

$$c = -T \frac{\partial^2}{\partial T^2} f(T, H)$$

LL-Bose gas: the exact solution:

- BA- wavefunction:

$$\psi_\chi\left(x_1, x_2, \ldots, x_N\right) = \sum_P A(P)\exp(i(\mathrm{k}_{P1}x_1 + \cdots + \mathrm{k}_{PN}x_N))$$

$$A(P) = C\epsilon(P)\prod_{j<l}(\mathrm{k}_{Pj} - \mathrm{k}_{Pl} + ic)$$

- Energy eigenvalues:

$$E = \frac{\hbar^2}{2m}\sum_{j=1}^{N}k_j^2,$$

- BA-equations:

$$\exp(\mathrm{i}k_j L) = -\prod_{\ell=1}^{M}\frac{k_j - k_\ell + \mathrm{i}\,c}{k_j - k_\ell - \mathrm{i}\,c} \quad j = 1\ldots N$$

Geometric Ansatz: the basic idea

- Change to Jacobi coordinates, which allows to remove the CM-coordinate;

- Change of coordinates to hyperspherical coordinates: radial component λ and the angular part $\vec{\theta} = \{\theta_1, \theta_2, ...\theta_{N-2}\}$.
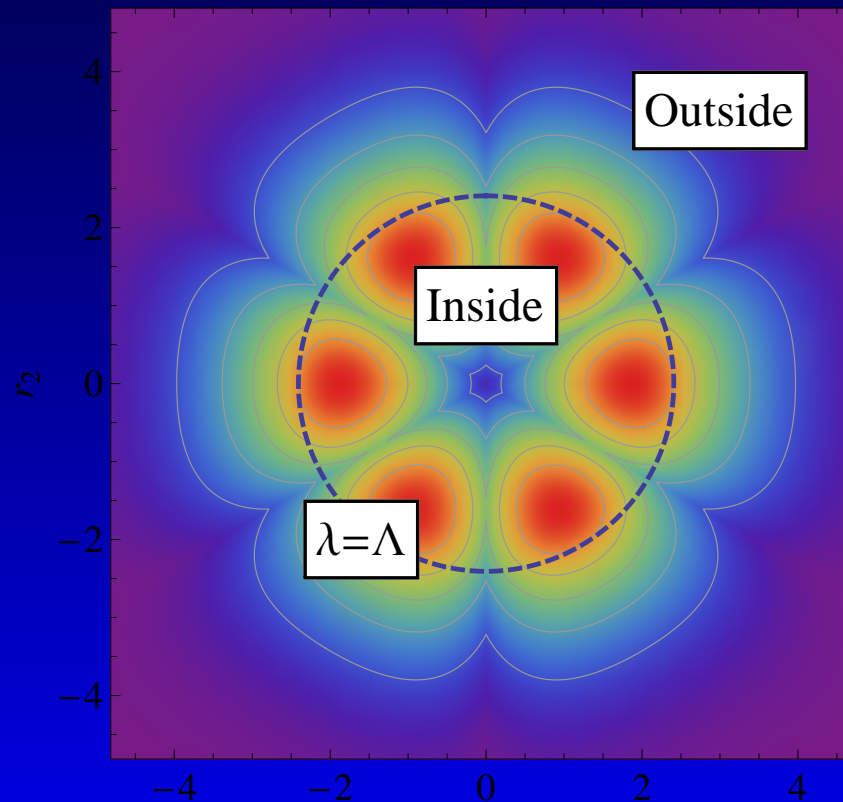
- The relative Hamiltonian now takes the form:

$$\hat{H}_{rel} = -\frac{\hbar^2}{2\mu}\nabla^2 + \frac{1}{2}\mu\omega^2\lambda^2 + c\sum_j \delta\left(d_j(\vec{\theta})\right).$$

For small λ, $\hat{H}_{rel}$ is approximately the one solved by the Bethe ansatz. For large λ the behaviour is dominated by that of a harmonic oscillator.

Variational principle: $E_{GS} \leq \frac{\langle \psi | H_{rel} | \psi \rangle}{\langle \psi | \psi \rangle}$,

Geometric Ansatz for the trial wavefunction:

$$\Psi(\lambda, \vec{\theta}) = \begin{cases} \psi_B\left(\vec{\kappa}, \lambda, \vec{\theta}\right) & \lambda < \Lambda \\ A(\vec{\theta}) \exp\left(-\alpha(\vec{\theta})(\lambda^2 - \Lambda^2)\right) & \lambda > \Lambda \end{cases} .$$

Schematic representation of $|\Psi|^2$ for $N = 3$. Λ determines the boundary between 2 regions: inside (Bethe ansatz) and outside (asymptotic harmonic oscillator). The colors range from purple to red indicating respectively lower values and higher values of $|\Psi|^2$.

Density Profiles

The equation of state can be reformulated within the local density approximation (LDA) by a replacement $\mu(x) = \mu(0) - \frac{1}{2}m\omega_x^2 x^2$ in which x is the position and ω_x is the trapping frequency, the total particle number and the polarization are given by:

$$
\begin{aligned}
\frac{N}{a_x^2 c^2} &= \int_{-\infty}^{\infty} \tilde{n}(\tilde{x})d\tilde{x}, \\
P &= \int_{-\infty}^{\infty} \tilde{n}_1(\tilde{x})d\tilde{x}/(N/(a_x^2 c^2)).
\end{aligned}
$$

Universal Ratios

In condensed matter, dimensionless ratios of quantities that take universal values can provide deep physical insights. Some examples include:

- Wiedemann-Franz ratio

- Sommerfeld-ratio

- Kadowaki-Woods ratio

- Korringa ratio

Why universal ratios are important?

- show that the same particles are responsible for the two different quantities that form the ratio;

- provide significant constraints on theories;

- demonstrate universality.

Wilson Ratio

- Dimensionless ratios of quantities that take universal values can provide deep physical insights.

- The Wilson ratio is defined as the ratio of the magnetic susceptibility χ to specific heat c_v divided by temperature.

- The Wilson ratio has recently been measured in a spin 1/2-ladder compound $(C_7H_{10}N)_2C_uB_{r2}$.

- Procedure: The main ingredients χ and c_v are obtained from the TBA-equations.